Science of the Total Environment 868 (2023) 161585

Contents lists available at ScienceDirect

Science of the Total Environment

journal homepage: www.elsevier.com/locate/scitotenv

Extensive assessment of climate change impacts on coastal zone paddy growth using multispectral analysis and hydrodynamic modeling

Samera Samsuddin Sah [a,b,d], Khairul Nizam Abdul Maulud [a,c,*], Othman A. Karim [a], Suraya Sharil [a], Zaher Mundher Yaseen [e,f]

[a] Department of Civil Engineering, Faculty of Engineering & Built Environment, Universiti Kebangsaan Malaysia, 43600 Bangi, Selangor, Malaysia
[b] Faculty of Chemical Engineering & Technology, Kompleks Pusat Pengajian Kejuruteraan Jejawi 3, Universiti Malaysia Perlis, 02600 Arau, Perlis, Malaysia
[c] Earth Observation Centre, Institute of Climate Change, Universiti Kebangsaan Malaysia, 43600 Bangi, Selangor, Malaysia
[d] Centre of Excellence Water Research and Environmental Sustainability Growth (WAREG), Universiti Malaysia Perlis, Kompleks Pusat Pengajian Jejawi 3, 02600 Jejawi, Perlis, Malaysia
[e] Civil and Environmental Engineering Department, King Fahd University of Petroleum & Minerals, Dhahran 31261, Saudi Arabia
[f] Interdisciplinary Research Center for Membranes and Water Security, King Fahd University of Petroleum & Minerals, Dhahran 31261, Saudi Arabia

HIGHLIGHTS

- Assessment for seawater encroachment on water quality (salinity & pH) was conducted.
- Spatial and hydrodynamic approaches were used for the growth of paddy trees.
- Two paddy seasons (May 2019-Jan 2020) of Kuala Kedah, Malaysia; were investigated.
- Results shows water salinity has a significant relationship with tidal variations.
- Three plant indices revealed a direct effect to the paddy crops and yields health.

GRAPHICAL ABSTRACT

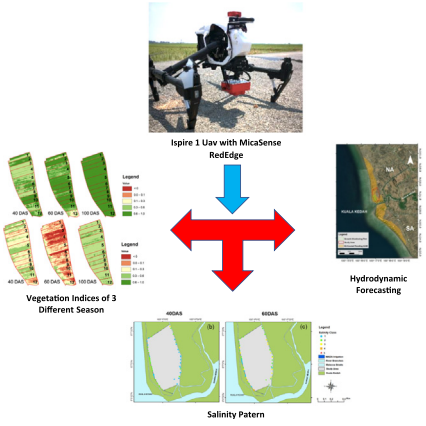

ARTICLE INFO

Editor: Fernando A.L. Pacheco

Keywords:
Food security
Hydrodynamics modeling
Multispectral analysis
Saltwater encroachment
Water quality

ABSTRACT

Global warming has led to sea levels raise (SLRs) and Malaysia is no exception to this problem. Especially for low-lying coastal areas including the Kuala Kedah area which is active in agricultural and fisheries activities. Farmers have had to bear up to 75 % of yield losses due to seawater breaches since 2016. Therefore, this study is designed to assess the impact of seawater encroachment on water quality through spatial technology approaches and hydrodynamic modeling related to the growth of paddy trees. The study was conducted during two different paddy cultivation seasons namely Season 1–2019 and Season 2–2019 which take place in the southwest and northeast monsoon in Kuala Kedah, Malaysia. The study involved three phases, which are the assessment of salinity and pH concentration levels, the assessment of the health of paddy crops through multispectral image analysis involving three plant indices (VI), namely Normalized Difference Vegetation Index (NDVI), Blue Normalized Difference Vegetation Index (BNDVI) and Normalized Difference Red Edge (NDRE), and finally, the assessment of the impact of SLR through the numerical method in MIKE 21 for hydrodynamic modeling considering two conditions that are without mitigation factor (K1) and with existing mitigating factor (K2). According to the findings, the salinity concentration trend is decreasing across the growth stage during Season 1–2019, whereas it is the contrary during Season 2–2019. It was discovered that during

* Corresponding author at: Earth Observation Centre, Institute of Climate Change, Universiti Kebangsaan Malaysia, 43600 Bangi, Selangor, Malaysia.
E-mail address: knam@ukm.edu.my (K.N. Abdul Maulud).

http://dx.doi.org/10.1016/j.scitotenv.2023.161585
Received 1 November 2022; Received in revised form 8 January 2023; Accepted 9 January 2023
Available online 19 January 2023

the study period for both tidal events, 73 % of the 44 sampling points in Season 1–2019, as opposed to just 3 % in Season 2–2019, were categorized as Class 4 and Class 5. Even though there were fluctuations throughout the observation, the pH reading is still within the allowed range of 6.5 to 9.0 for the estuary area. Following that, the ANOVA analysis proved that salinity concentration a statistically significant difference with tidal variations and pH levels. Moreover, the multispectral image analysis findings revealed that the VI value was correlated with both the yield and the health of the rice crop, with R-square values of 0.842 compared to 0.706 and 0.575 for NDVI and BNDVI values, respectively. It confirmed that NDRE granted a more accurate and reliable measurements. Additionally, the hydrodynamic simulation results demonstrated that, if the mitigation factors were considered in the modeling, overflow seawater to the mainland could be reduced by up to 20 %, reducing the impact of coastal flooding on the local area as well as the nearby rice cultivation area. Ultimately, these three elements—water quality, vegetation index, and hydrodynamic modeling—can assist in identifying the underlying cause of the problem and develop short and long-term solutions.

1. Introduction

Agriculture is a branch of industry that plays an important role in supplying food resources for any country (Maghrebi et al., 2020; Salman et al., 2021). Land use data for Malaysia shows that more than five million hectares of land are classified as agricultural areas, as recorded by Department of Town and Country Planning Malaysia (2018) and paddy crops are the third largest crop in Malaysia after oil palm and rubber plantations (Department of Agriculture Malaysia, 2020). However, according to the statistics of rice production released by Department of Agriculture Malaysia (2020), the total rice yield in Kedah decreased by 15 % in 2019 with only 560 metric tons recorded compared to 660 metric tons in 2016. Radanielson et al. (2018a) and Reddy et al. (2017) reported that if the electric conductivity (EC) >2 dS/m, the reduction in paddy yield can reach up to 1 ton per hectare.

Generally, paddy cultivation in Malaysia, which involves flooded paddy type, is highly dependent on the water quality level especially salinity concentration and water pH which has a significant impact on the growth rate of this crop (Dam et al., 2019; Reddy et al., 2017). The value of the salinity concentration of water can be measured by the value of electrical conductivity (EC). As reported by Grieve et al. (2012) and Phogat et al. (2010), if the EC value is >2 dS/m, the yield of paddy will decrease by up to 1 ton of rice per hectare. In addition, the yield of paddy will continue to decrease by up to 50 % if the EC reading is >6 dS/m, but the durability of the paddy tree also depends on the growth stage of the paddy crop (Radanielson et al., 2018a, 2018b; Thu et al., 2017). At the seeding stage, the paddy sapling may die if the EC value reaches 10 dS/m. While at the reproductive stage, the yield of rice will be reduced by up to 90 % if the EC value reaches 3.5 dS/m.

In terms of water pH level, a lower pH value is better for the plant to produce higher concentrations of leaf chlorophyll, and thus, provide a better amount of yield (Liu et al., 2016). In accordance with Kahimba et al. (2016), the normal pH range of irrigation water for agricultural purposes is from 6.5 to 8.4. However, the pH of the water does not cause a change in the pH of the soil if the soil is a type of clay compared to sandy soil. This is because clay is a type of soil that has excellent buffer ability (McCauley et al., 2017; USDA, 1994).

Some studies have found that increased salinity rates due to climate change and human activities (Khanom, 2016) in the irrigation system of paddy farming can have a negative impact on the growth of the crop (Ahmed and Haider, 2014; Baten et al., 2015; Fraga et al., 2010; Gain et al., 2004; Phogat et al., 2010; Reddy et al., 2017). The release of river water into the sea and the variation of tides are among the factors that cause the problem of sea water invasion in the estuary (Cheng et al., 2012; Khojasteh et al., 2020). According to Garcés-Vargas et al. (2020) and Uncles and Stephens (2011), authors indicated that tidal variation can affect the level of seawater intrusion up to tens of kilometers into the river and cause an increase in salinity levels due to the presence of sea water in rivers and irrigation systems. Furthermore, Garcés-Vargas et al. (2020) stated that the intrusion of seawater into coastal areas is a factor resulting in a reduction in agricultural yields in addition to pest infestation, which was also reported by Herman et al. (2015). Therefore, hydrodynamic modeling can provide a clearer and more accurate picture of coastal flooding due to SLRs in the affected areas in the long term. This hydrodynamic model is a tool used to monitor and predict coastal conditions based on a numerical analysis that is part of the physical model test (Belibassakis and Karathanasi, 2017). In the commercial market, there are different types of hydrodynamic software used in coastal studies (Iglesias et al., 2019), involving one-dimensional (1D), two-dimensional (2D) or three-dimensional (3D) modeling. Each model has a different capacity according to the tidal flow that has different numerical difficulties, such as complex geometry, large-sized domains, and independent surface determination, which represents the boundary condition of a study area (Suárez-López et al., 2019).

A 2D numerical model was used on flows with more complex geometry, or when there are some strong velocity variations in cross-section, such as vortex and re-circulation flow (Suárez-López et al., 2019). It was able to give a more accurate description than the 1D model. Moreover, this model is capable of providing accurate results in case of flow inconsistency. The Reynolds equation of average depth is used in this model by defining the roughness of the base with the value of Manning or Strickler (Glock et al., 2019). Among the widely used 2D numerical models are Hydro_AS-2D, MIKE 21, Delft3D-Flow and TELEMAC-2D. MIKE 21 is an unstructured hydrodynamic model which has proven to be the most efficient model when run on multiple cores (Symonds et al., 2017) as well as producing more accurate results especially for modeling in estuaries and rivers (Fattah et al., 2018; Parsapour-moghaddam et al., 2018). Meanwhile, spatial technology is seen to be gaining popularity in agriculture in monitoring the growth of a crop. This technology can be used to monitor the health of the paddy tree and estimate its crop yield (Yeom et al., 2021), detect problems related to the irrigation system (Kamruzzaman et al., 2020; Norasma et al., 2018) and water quality levels (Tack et al., 2015), as well as producing dynamic and informative crop monitoring maps (Xiao et al., 2021; Yeom et al., 2021; Zhang et al., 2017).

Additionally, the vegetation index (VI) is a spectral transformation of two or more bands developed to increase the value of the properties of plants and allow reliable spatial and temporal comparison of terrestrial photosynthesis activity and variations of canopy structures, as discovered by Huete et al. (2002). Most of the VIs have similar functions and use a reverse relationship between red reflection and NIR that correlates with healthy green plants (Liu et al., 2019; Lu and Zhuang, 2010; Migliavacca et al., 2018; Yebra et al., 2013), such as *Normalized Difference Vegetation Index* (NDVI) (Rouse et al., 1973), *Blue Normalized Difference Vegetation Index* (BNDVI) (Wang et al., 2007), and *Normalized Difference Red Edge* (NDRE) (Buschmann and Nagel, 1993). Based on the reported literature, there is a massive interest in studying the SLRs effects on the coastal layout. Particularly, for regions highly interacted with seashore such as Malaysia.

Therefore, this study is conducted to assess the impact of seawater encroachment on water quality through spatial technology approaches and hydrodynamic modeling related to the growth of paddy trees. The hydrodynamic modeling of MIKE 21 as well as water quality in paddy crop areas especially for salinity and water pH parameters, were studied. In addition, this research supported by the use of multispectral image analysis capable of translating plant conditions using a vegetation index. Furthermore, the

null hypothesis of this study was formed, which is that seawater encroachment has no significant effect on the water's salinity concentration and pH level. Meanwhile the alternative hypothesis is that seawater has a significant effect on the water's salinity concentration and pH level. ANOVA was used for the statistical analysis, with a significance level of 5 %.

In addition, this study is planned and carried out in accordance with the existing condition of the study area, which includes a number of scopes and limitations. Firstly, the salinity level and water pH are the first two water quality parameters that have been closely examined in this study. Based on the literature reviewed, it was thought that these variables had a significant impact on the growth of the paddy plants. Moreover, three vegetation indices—NDVI, NDRE, and BNDVI—are evaluated and compared in order to discover the best indicator that could accurately represent the healthiness of paddy plants. Besides, this study specifically observed the effect of splashing seawater into the nearest surface water bodies without focusing on other aspects like diseases or groundwater.

In brief, this study began with the procedure of identifying sampling points for water sample collection throughout three periods, namely 10 days after sowing (DAS), 40 DAS, and 60 DAS. Then, the aerial image acquisition is planned and executed in accordance with the growth stage of the paddy plants using a drone equipped with multispectral camera. The acquisition process begins from 40 DAS, 60 DAS, and 100 DAS, which representing the vegetative, flowering, and maturity stages, representing the vegetative, flowering, and maturity stages. Subsequent, by using the Agisoft Metashape software, the captured aerial images are analyzed and transformed into a raster image with vegetation index values. In addition, the collection of secondary data from the local agency, namely the National Water Research Institute of Malaysia (NAHRIM), is carried out to perform the hydrodynamic modeling using MIKE Zero and MIKE 21 software. This secondary data is used as a baseline for the purpose of calibrating and verifying simulated models. Lastly, the outcomes from each phase—water quality, image processing, and hydrodynamic modeling were assessed together.

2. Methods and materials

This study was conducted in a 30-ha rice cultivation area located approximately 200 m from the coastline of Kuala Kedah, Malaysia as shown in Fig. 1 and this area is regulated by a statutory body known as the Muda Agricultural Development Authority (MADA). There is a river that is the link or used as a small and medium-sized boat route for fisheries activities in the area, which is known as Sungai Kedah with the coordinates 6° 06′ 27" N, 100° 17′ 3.12" E. Most of the residents in Kuala Kedah are intensively involved in paddy farming activities. This study was conducted in 2019 and involved two paddy planting seasons, namely Season 1–2019 and Season 2–2019. Season 1–2019 involved paddy planting activities ranging from the plot preparation process to harvesting activities carried out from May to August 2019, while October 2019 to January 2020 was the planting period for Season 2–2019.

In total, the study had three main phases: Phase 1 involved the collection of water quality data focusing on the value of salinity concentration and pH for each water inlet and outlet for each paddy plot involved. Phase 2 adopted on the observation of aerial images using an unmanned aerial aircraft (UAVs) for an area of 10 ha covering 12 paddy plots located closest to the coastline. Finally, Phase 3 involved hydrodynamic simulations aimed to predict and identify areas with potential coastal flooding due to rising sea levels.

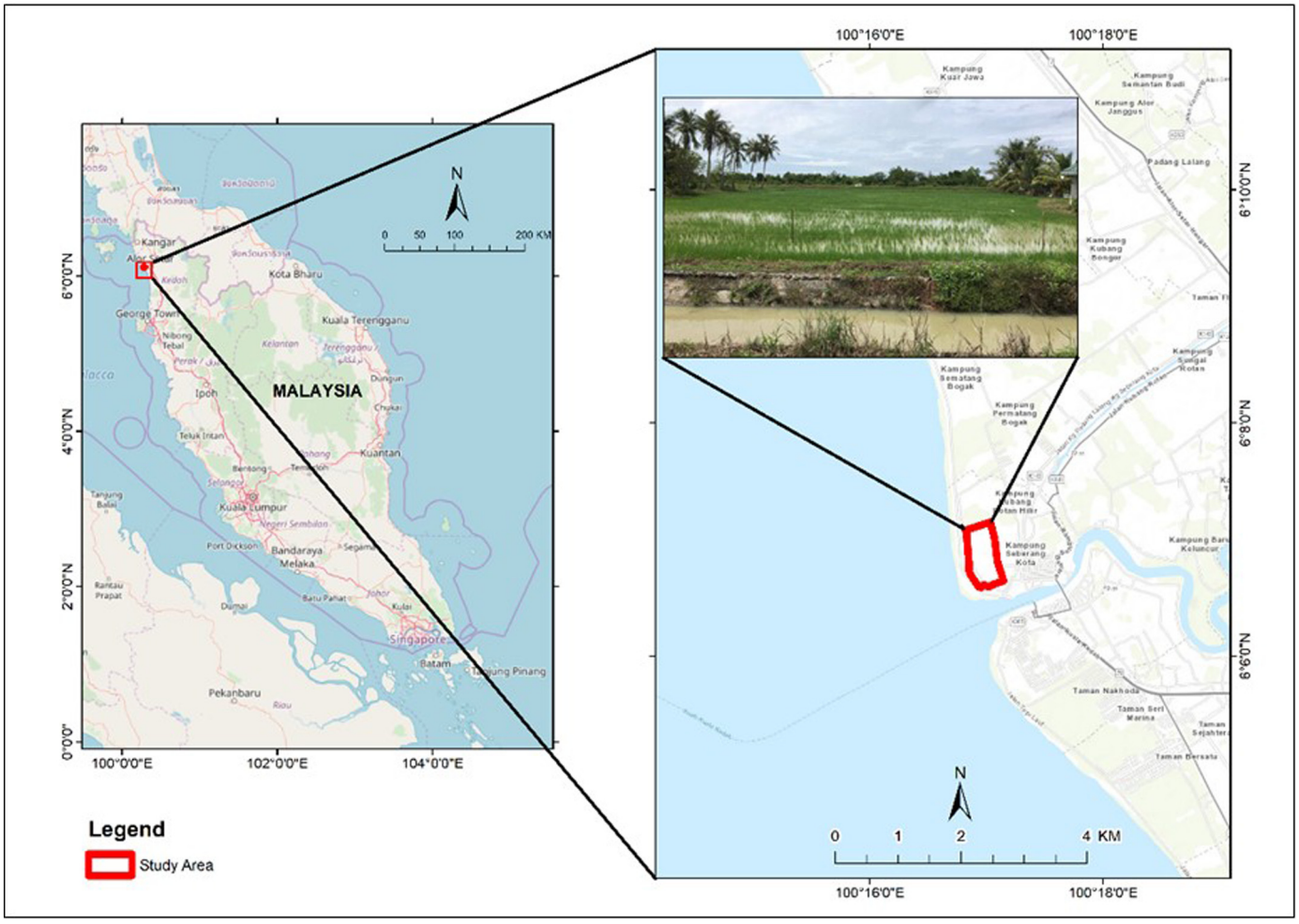

Fig. 1. Study area in Kuala Kedah, Malaysia.

Table 1
General range of water salinity concentrations by category.

Class	Concentration (ppm)	Description
1	0–456	Very Low
2	457–700	Low
3	701–1100	Moderate
4	1100–1500	High
5	> 1500	Very High

Source: Abrol et al., 1988; Prince, 2019.

In Phase 1, water salinity concentration and water pH were two water quality parameters studied directly by testing water samples collected from the field in the period of May to July 2019 and October to December 2019, respectively, for Season 1–2019 and Season 2–2019. Each sample collected at 10 DAS, 40 DAS and 60 DAS per season was analyzed and classified based on the general range of water salinity concentration as set out in Table 1, which is also used as a guideline by Abrol et al. (1988) and Prince (2019). Fig. 2 shows a clear picture of the position of 44 water sample points, main irrigation, and MADA irrigation canals in the study area. There is a MADA water pump house located about 1 km from the tidal gate in the downstream area which serves as a platform to flow the river water to the upstream area of the tributary.

Phase 2 was accommodated the data process from June 2019 to January 2020 involved the process of aerial image observation for a period of 40 DAS, 60 DAS and 100 DAS using an unmanned aerial vehicle (UAV) equipped with multispectral camera. For every point on the flight path, this multispectral camera can capture five black-and-white images, specifically representing the Red (R), Blue (B), Green (G), Near-Infrared (NIR), and Red Edge bands, as shown in Fig. 3.

Each aerial image had been recorded, analyzed using *Agisoft Metashape* and ArcGIS software to translate crop conditions, and stored as a Geotiff image that has a value of VI. For this study, three VIs - NDVI, NDRE, and

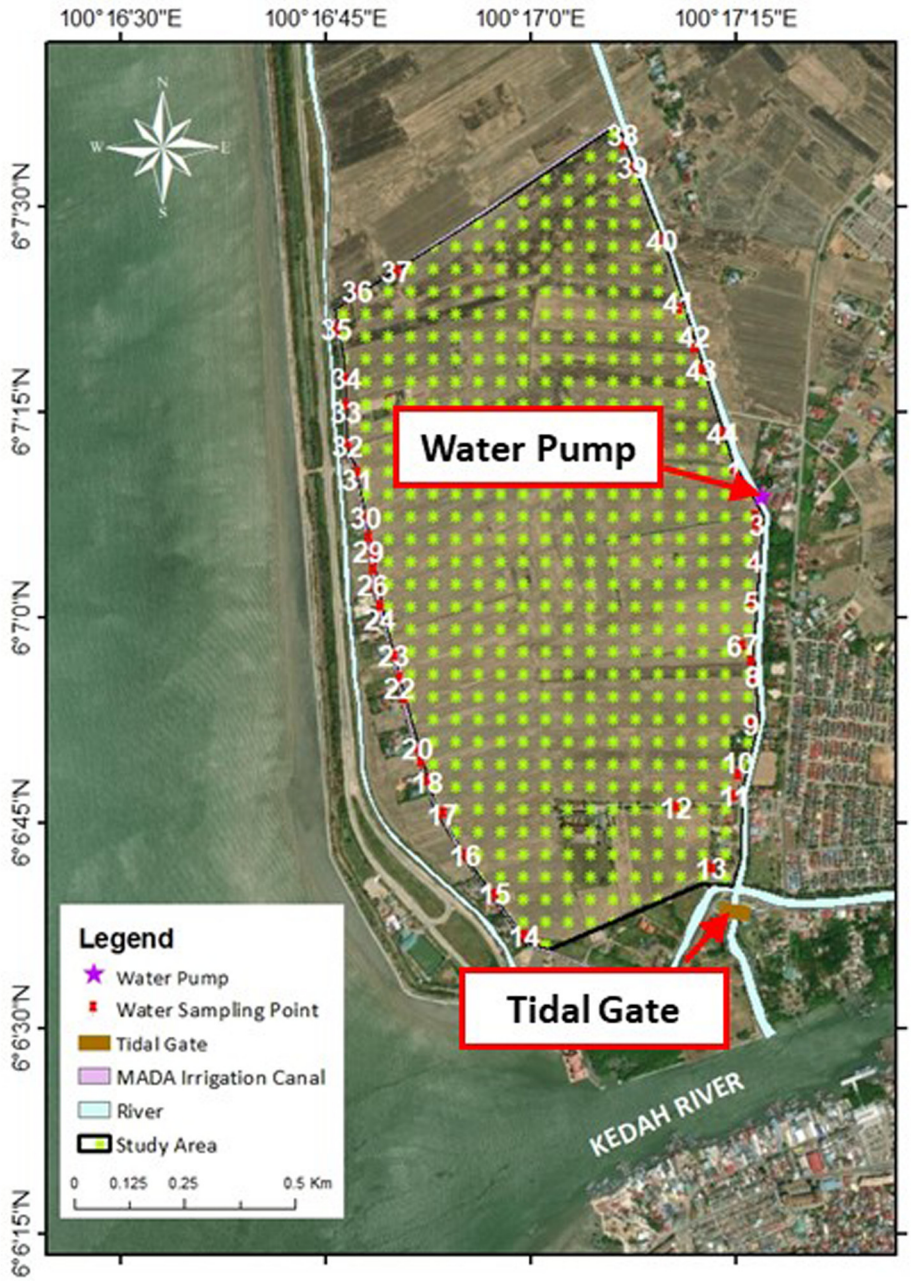

Fig. 2. Sampling point location and irrigation system in the study area.

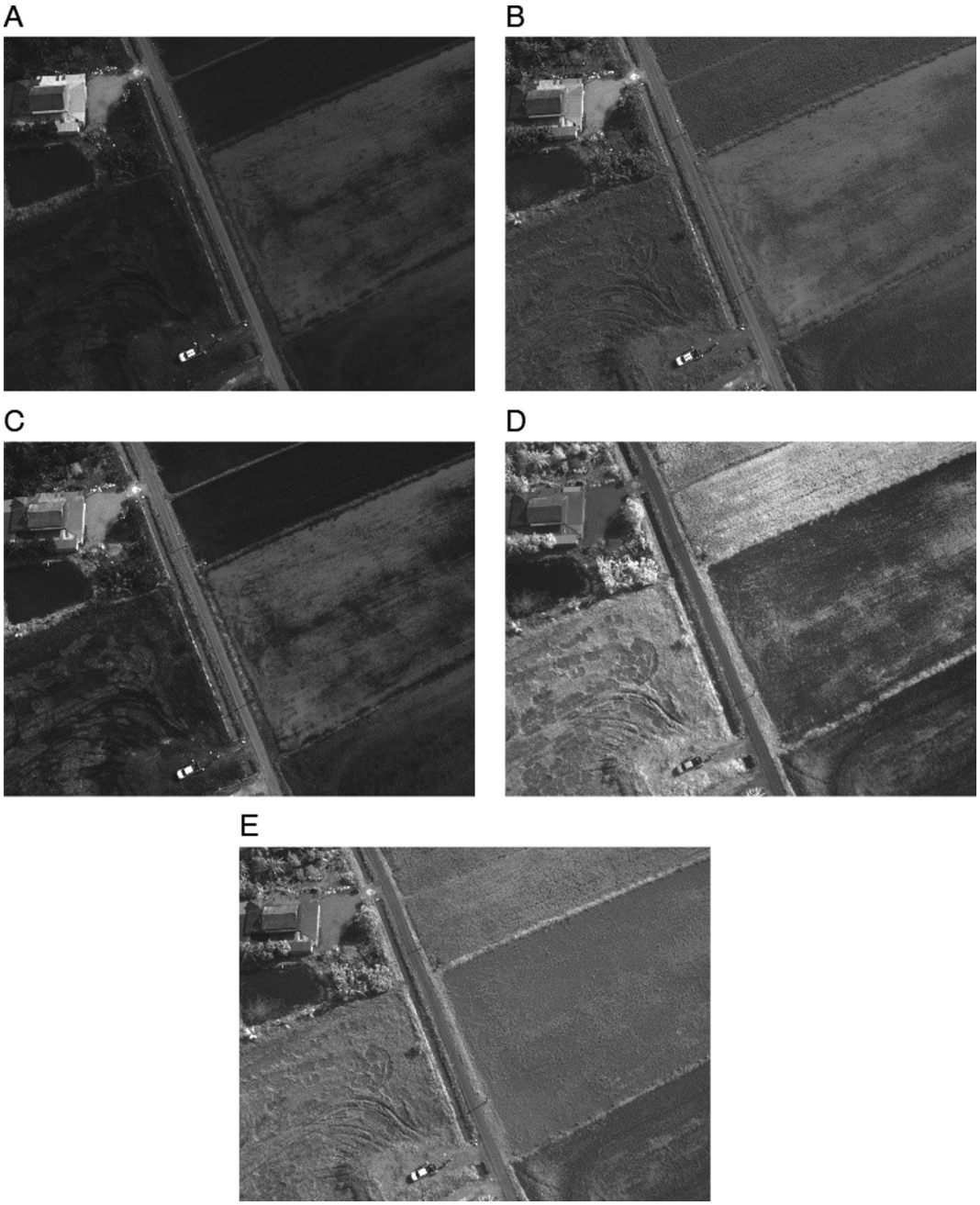

Fig. 3. Example of multispectral images were captured for 5 different bands, which are (a) Red, (b) Green, (c) Blue, (d) Near-infrared, and (e) Red edge.

BNDV - were employed in accordance with the formula in Table 2. These three VIs have the capacity to represent a crop condition. Next, each VI value was classified into several categories as stated in Table 3 and analyzed according to the observed rice crop plot.

Finally, Phase 3 involved a hydrodynamic simulation process that uses secondary data obtained from NAHRIM for the study area. This process began with identifying the study area and determining the boundaries of the study area. Then, the border information was stored and uploaded in the MIKE Zero software to generate the mesh. This mesh file was then uploaded in the MIKE 21 Flow HD module. After all the necessary information was uploaded, the simulation process began by performing the calibration and verification of this model. The calibration value was determined using the average squared difference between the measured and predicted values named as the Root Mean of Square Error (RMSE). The RMSE value reflects the good performance of the model by assessing the least balance between the two data sets (Abd Rahim et al., 2021; Neill and Hashemi, 2018). The following is the RMSE formula used.

$$RMSE = \sqrt{\frac{1}{n}\sum_{i=1}^{n}(S_i - O_i)^2} \quad (1)$$

Table 2
Vegetation index formulation for NDVI, NDRE and BNDVI.

Vegetation Index (VI)	Calculation index	Source
Normalized Difference Vegetation Index	$NDVI = \frac{NIR - Red}{NIR+Red}$	(Rouse et al., 1973)
Normalized Difference Red Edge	$NDRE = \frac{NIR - RedEdge}{NIR+RedEdge}$	(Buschmann and Nagel, 1993)
Blue Normalized Difference Vegetation Index	$BNDVI = \frac{NIR - Blue}{NIR+Blue}$	(Wang et al., 2007)

Table 3
Categories based on the value of the vegetation index (VI).

Class	Index Value	Description
1	< 0	No Vegetation
2	0 to 0.1	Low Vegetation Density
3	0.1 to 0.3	Moderate Vegetation Density
4	0.3 to 0.6	High Vegetation Density
5	0.6 to 1.0	Very High Vegetation Density

Source: Jesslyn, 2015; Giacomo and David, 2018; Zaitunah et al., 2018; Hashim et al., 2019.

Table 4
Calibration values of coastal hydrodynamic parameters.

Parameter	Calibration value
Water Level	<10 %
Current Speed	<20 %
Current Direction	<20 Degree

Source: Department of Irrigation and Drainage Malaysia, 2013.

where O_i is the observation data, S_i is the model data for a variable, and n is the number of observation data analyzed. Table 4 tabulated the guidelines for coastal hydraulic modeling studies issued by the Department of Irrigation and Drainage Malaysia (2013) to analyze the accuracy and reliability of modeling results using the RMSE statistical analysis approach (Mohd et al., 2018a, 2018b). The verification process was done by making comparisons with the observed data. Once this process was completed, the coastal flood analysis was done by assessing and predicting the level of seawater advance to the mainland and affected areas due to the increase in sea water levels in 2012 used as baselines, and subsequently forecasts in 2020, 2050, and 2100.

3. Results

In this section, modeling results reflection was reported for the designed methodology of the hypothesized research aims. Rainfall distribution factors, average temperature, and tidal events have been identified as factors that can influence the environmental conditions in the study area, especially for the level of salinity concentration in the water in the paddy crop plot.

Table 5
Distribution by concentration class for 44 water samples.[a]

Class	10 DAS				40 DAS				60 DAS			
	S1 2019		S2 2019		S1 2019		S2 2019		S1 2019		S2 2019	
	HT	LT	HT	LT	HT	LT	HT	LT	HT	LT	HT	LT
1	–	–	34	32	10	8	21	18	32	44	9	19
2	–	1	10	11	21	21	22	23	12	–	21	12
3	15	14	–	1	10	13	1	3	–	–	13	13
4	21	24	–		3	2	–	–	–	–	1	–
5	8	5	–		–	–	–	–	–	–	–	–

Note: HT = high tide; LT = low tide; S1 = Season 1; S2 = Season 2.
[a] Water samples classification according to water salinity and days after sowing (DAS).

Based on preliminary monitoring and analysis of rainfall distribution patterns and average temperatures in the study area as shown in Fig. 4, it was found that the average rainfall was recorded at 129 % higher in Season 1–2019 than the average rainfall in Season 2–2019. According to the results of this consolidation, Season 1–2019 is classified as the rainy season, while Season 2–2019 as the dry season.

In addition, the pattern of tidal events in the study area was also monitored for the same period with reference to the 2019 tidal schedule book published by the National Hydrographic Centre of Malaysia. The maximum sea level height was recorded on May 19, 2019 and July 04, 2019, with a height of 3.11 m in Season 1–2019 and 3.18 m on October 29, 2019 during Season 2–2019. Meanwhile, the minimum height was as low as 0.24 m on May 05, 2019 and 0.04 m on October 28, 2019, for Season 1–2019 and Season 2–2019, respectively. Next, the analysis of the water sample shows the salinity concentration readings for each point classified according to the level of salinity concentration as summarized in Table 5. It was found during periods 10 and 40 DAS during Season 1–2019, 66 % and 7 % of the water samples tested were classified in Class 4 and Class 5 with salt concentration values exceeding 1100 ppm for both tidal events. While for Season 2–2019, only 3 % of the total water samples were classified as Class 4 during the tide event within the 60 DAS period.

Figs. 5 and 6 show the distribution of sample points according to the salinity concentration class for the entire study area during Season 1–2019 and Season 2–2019. Generally, salinity concentrations were relatively uniform throughout the study area at 10 DAS for both tidal events in Season 1–2019. Then, at 40 DAS the value of salinity concentration decreased

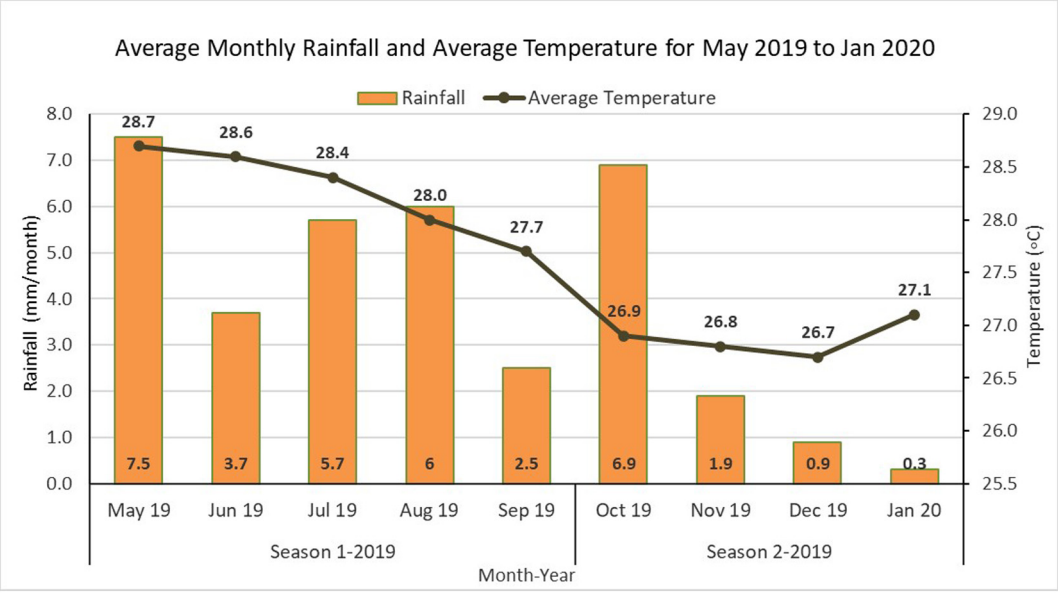

Fig. 4. Distribution of average monthly rainfall and average temperature for May 2019 to January 2020.

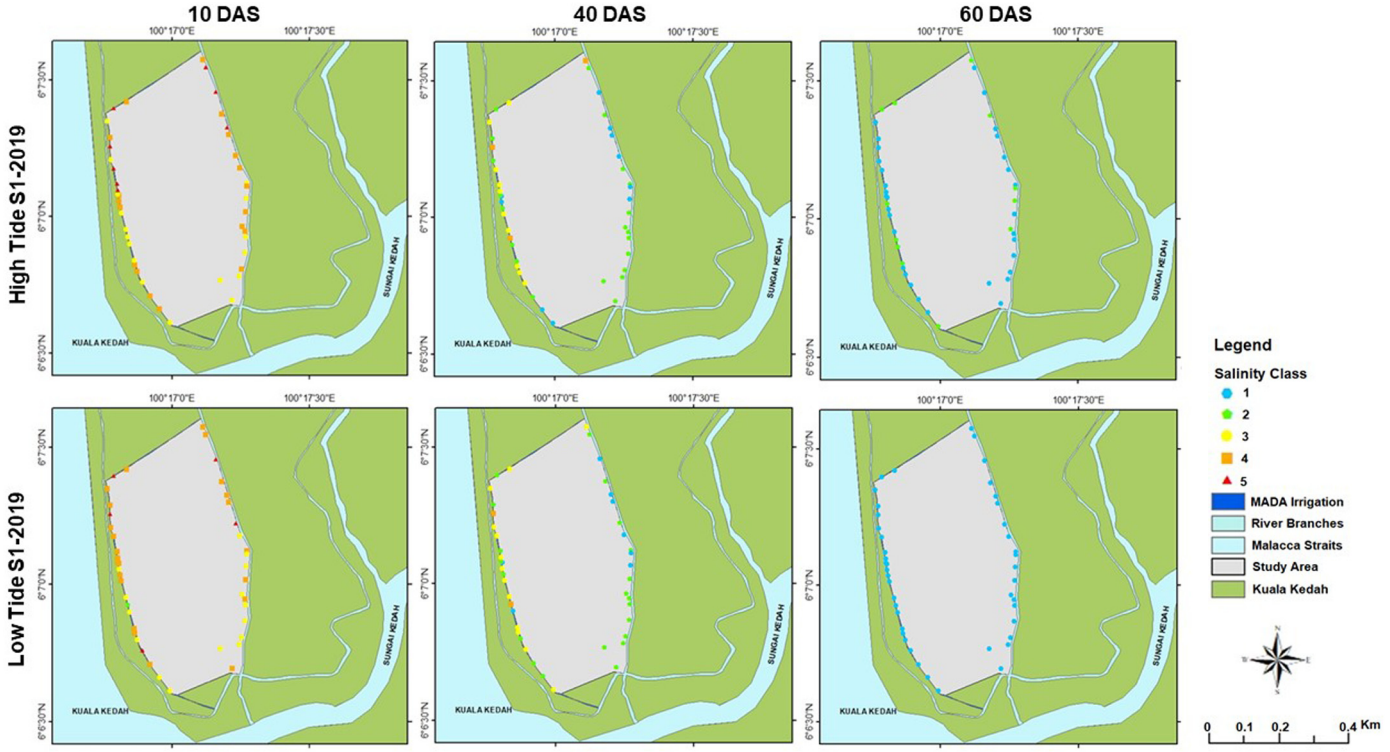

Fig. 5. The level of salinity concentration by class during the occurrence (a), (b), (c) of the tide and (d), (e), (f) of the receding waters for the three stages of rice growth during Season 1–2019.

and was concentrated in the part closest to the coastline. During the 60 DAS period, all sample points that showed a low salinity concentration of <700 ppm were categorized in Class 1 and Class 2 for both tidal events. While for Season 2–2019, the distribution of salinity concentration was dominated by Classes 1, 2 and 3 for both tidal events during the period of 10 and 40 DAS. Only one sample point i.e., point 14, was recorded in Class 4 at 60 DAS during the tide event.

Later then, pH values were plotted using a box plot based on the paddy growth period for both tidal occurrences in Season 1–2019 and Season 2–2019, as seen in Figs. 7 and 8. Season 1–2019 showed a fluctuation

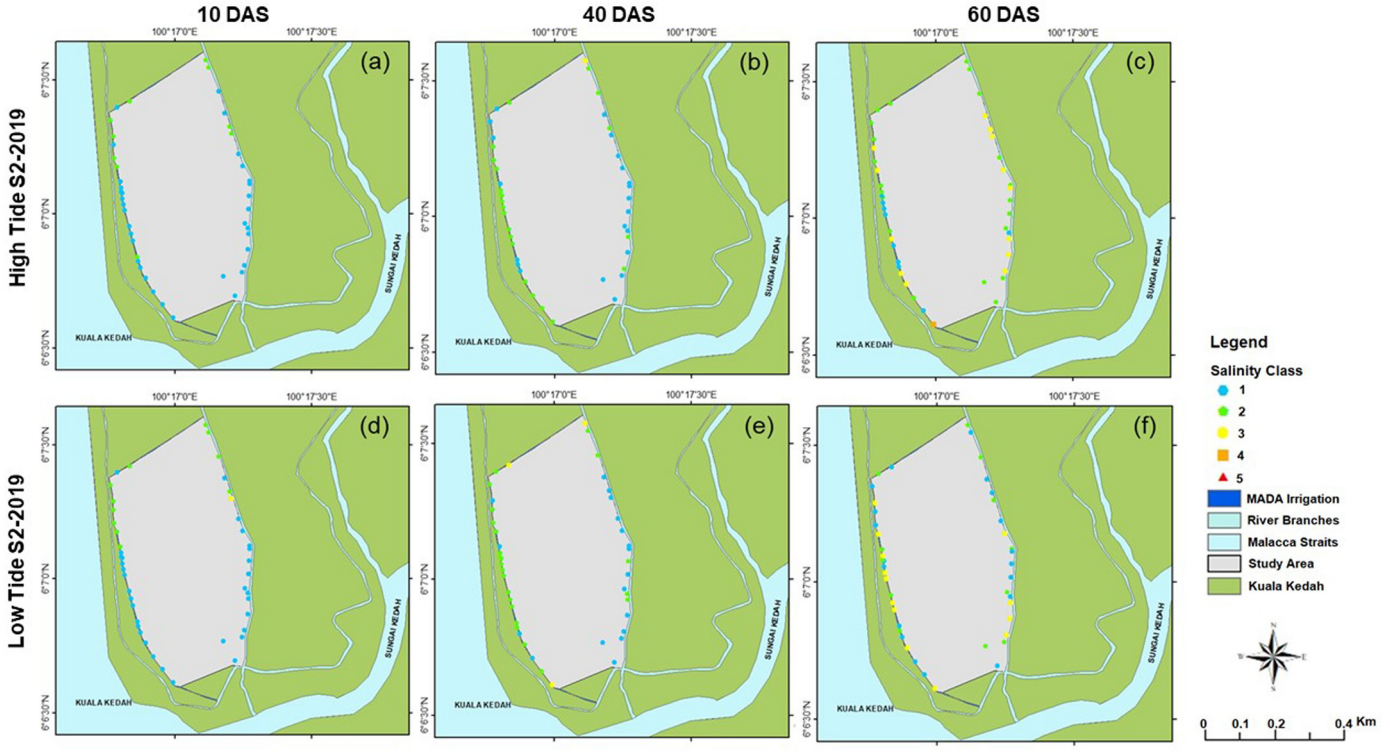

Fig. 6. Salinity concentration level by class during occurrence (a), (b), (c) tide and (d), (e), (f) low tide for the three stages of rice growth during Season 2–2019.

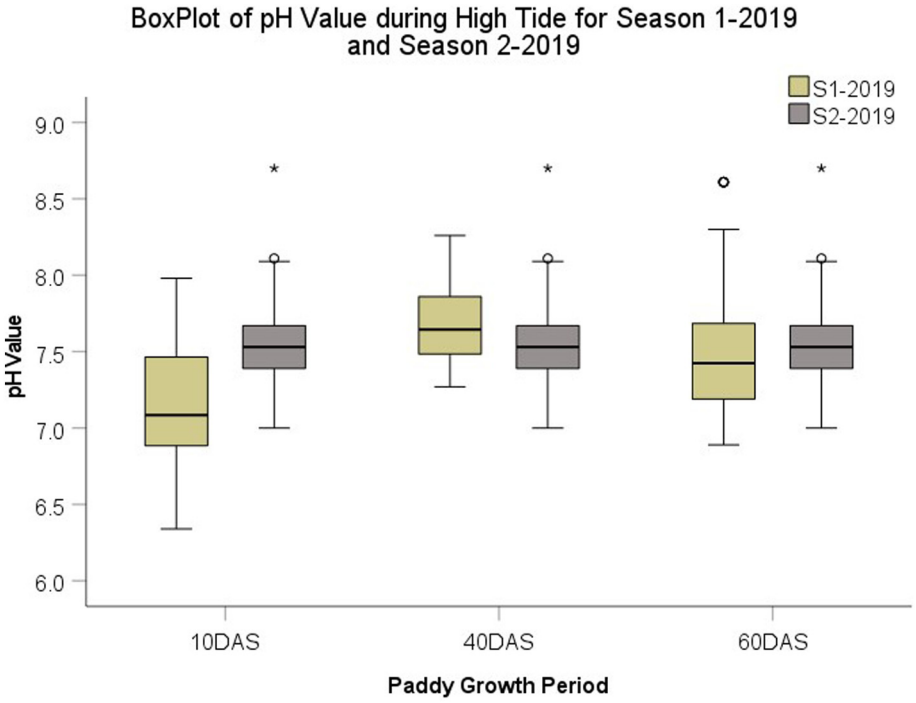

Fig. 7. Boxplot of pH values during high tide events for Season 1–2019 and Season 2–2019.

pattern in the periods of 10 DAS, 40 DAS, and 60 DAS for both tidal events, whereas Season 2–2019 shows a contrary trend, with pH levels reported as more stable and consistent during paddy plant development. During Season 1–2019, 75 % of sampling points recorded a pH value of <7.5 during high tide and also during low tide at 10 DAS and these values increased and approached 8.0 at 40 DAS and eventually dropped back to 7.5 and below. On the other hand, the pH values during Season 2–2019 showed that 75 % of the pH value was 7.7 for both tidal events. However, these boxplots can only represent graphically the spread of the pH data but cannot be easily interpreted the relationship between tidal events and pH values.

Table 6 shows the distribution of pH readings by class for both seasons. During the 10 DAS period in Season 1–2019, three samples from the water samples tested were classified in Class 1 with a pH value of <6.5 for both tidal events. However, there were two samples that recorded a pH value in Class 3, which is low tide at 40 DAS and high tide at 60 DAS. While for Season 2–2019, only one sample was classified as Class 3 during the tide event in the 10 DAS period. The rest of the time, the pH values of the other sample points showed a normal reading from 6.5 to 8.4.

While the multispectral analysis involved 12 paddy plots located about 200 m from the coastline, as seen in Fig. 9, which shows the layout of the

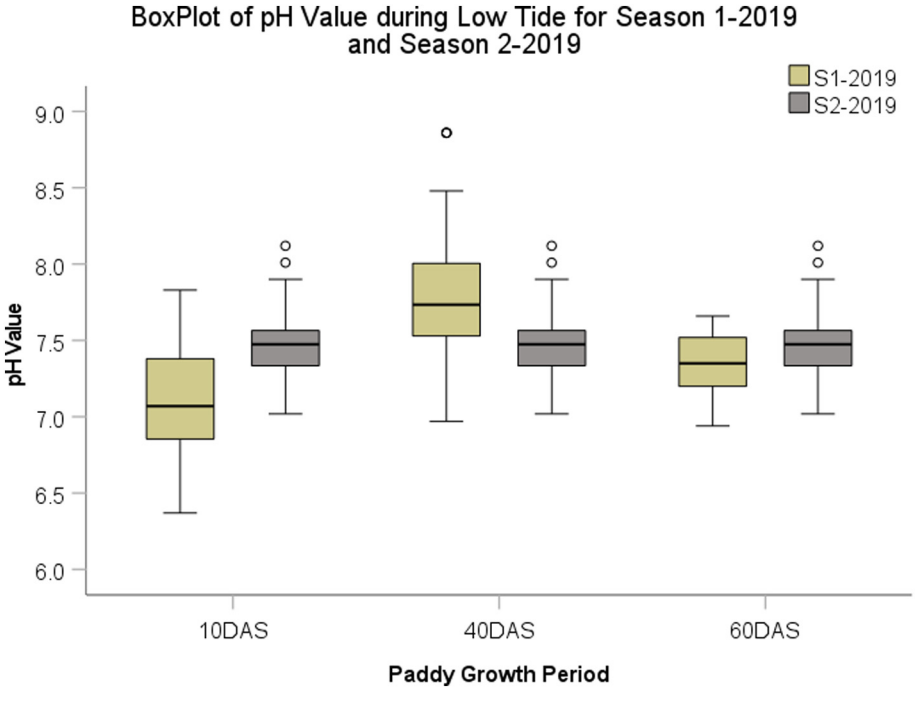

Fig. 8. Boxplot of pH values during low tide events for Season 1–2019 and Season 2–2019.

Table 6
Distribution by pH class of 44 water samples.[a]

Class	pH range	10 DAS				40 DAS				60 DAS			
		S1 2019		S2 2019		S1 2019		S2 2019		S1 2019		S2 2019	
		HT	LT	HT	LT	HT	LT	HT	LT	HT	LT	HT	LT
1	< 6.5	3	3	0	0	0	0	0	0	0	0	0	0
2	6.5–8.4	41	41	43	44	44	42	44	44	42	44	44	44
3	> 8.4	0	0	1	0	0	2	0	0	2	0	0	0

Note: HT = high tide; LT = low tide; S1 = Season 1; S2 = Season 2.
[a] Water samples classification according to potential of hydrogen and days after sowing (DAS).

plots involved in the study area of 10 ha. These plots are divided according to the name of the owners registered in MADA as well as in Beras Nasional.

The rice yield data for each paddy plot involved in this study was obtained from the two agencies. Fig. 10 shows the rice yield for each plot during Season 1–2019 and Season 2–2019. Based on this diagram, paddy yields are seen to be higher in Season 2–2019 compared to Season 1–2019 for each plot and plot-4 is the largest plot with an area of >3 ha. Meanwhile, the highest rice yield of almost 3500 kg/ha and 4500 kg/ha was recorded on plot-3 for the first and second seasons, respectively.

Fig. 11a and b showed the graph of vegetation index (VI) by plot for Season 1–2019 and Season 2–2019 as well as the paddy yield. During Season 1–2019, the average rice production for 12 paddy plots was 2345 kg per hectare compared to the 2795 kg per hectare recorded for Season 2–2019. From the perspective of VI, the value of each of these indices was averaged to represent the state of each plot. NDRE has the lowest values with average values of 0.347 and 0.288, respectively. For Season 1–2019 and Season 2–2019, which are categorized as Class 4 (High Vegetation Density) and Class 3 (Moderate Vegetation Density). Meanwhile, NDVI and BNDVI are in Class 5 (Very High Vegetation Density) with average values of 0.611 and 0.707, and 0.633 and 0.665, respectively, for Season 1–2019 and Season 2–2019. Subsequently, to get a clearer picture, mapping each VI using a color range as the presented in Table 2 was done for both seasons. Each VI value indicates an increase for each stage of rice growth. Overall, Fig. 12 shows that the value of VI in the second season is better than the first season of the twelve plots observed.

Fig. 13a, b and c showed the distribution of the area of each VI according to the rice plot. During the 60 DAS in Season 1–2019, 60 % of

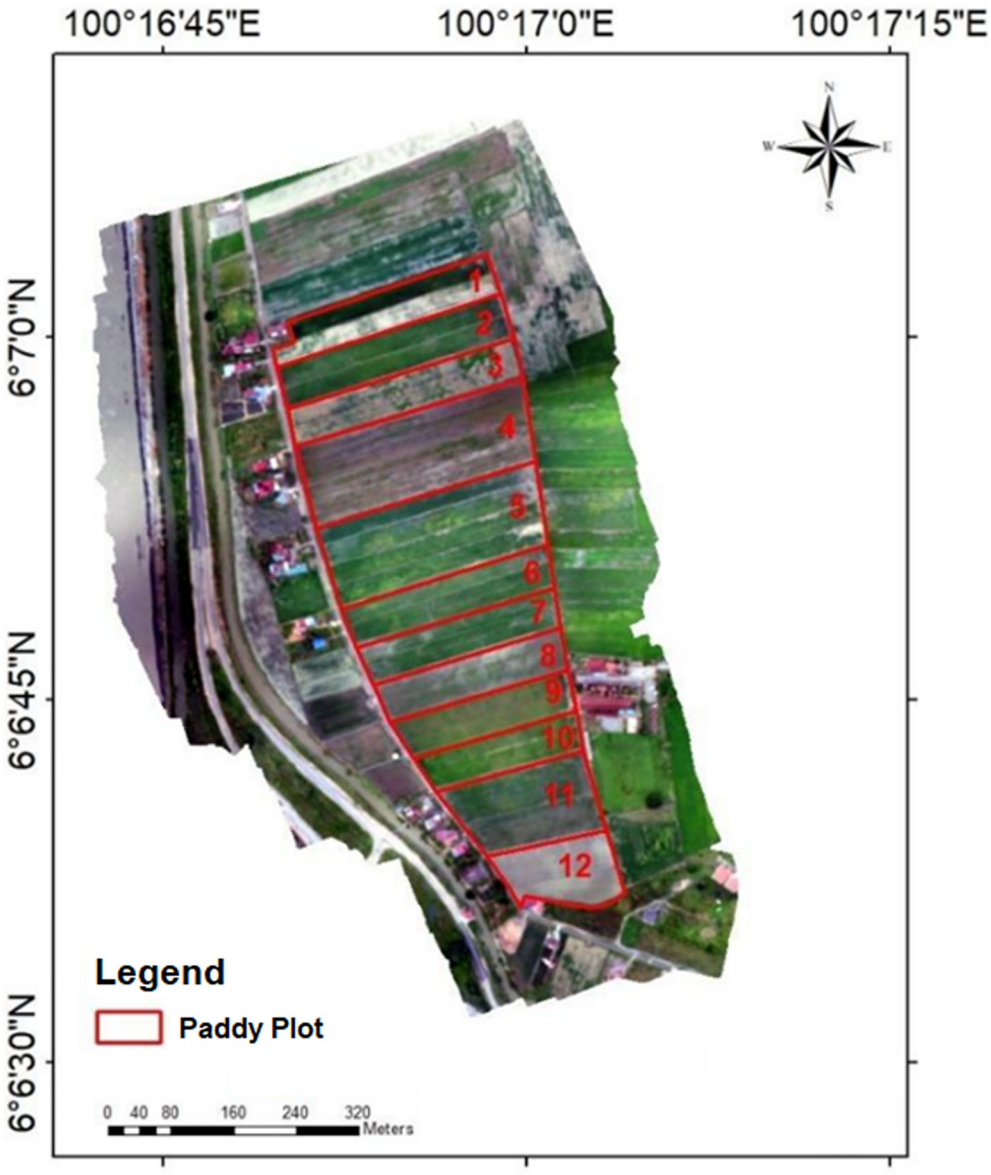

Fig. 9. Layout of 12 observed rice plots.

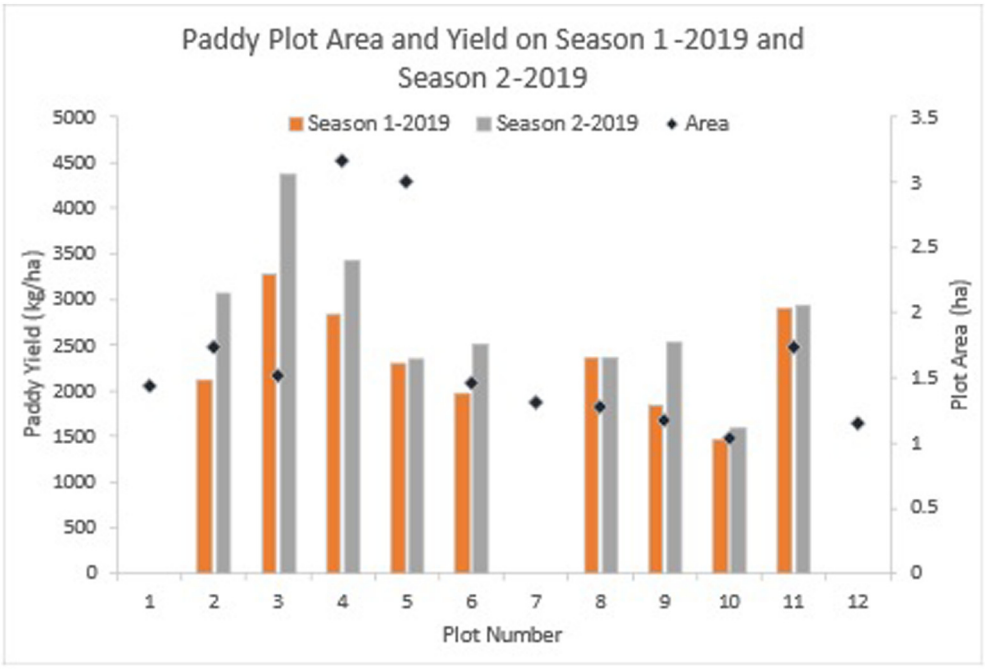

Fig. 10. Paddy yield by plot and plot area for Season 1–2019 and Season 2–2019.

the total plot-12 area was classified as Class 3, which has a moderate vegetation density of NDVI and BDNVI represented by blue, as illustrated in Fig. 12 (a) and (b), respectively. However, for the NDRE index value as seen in Fig. 13 (c), the majority of plot area 12 is categorized as Class 2, which has a low vegetation density represented by yellow.

Results for Season 2–2019, at 60 DAS, plot-3 showed a relatively low index value with almost 30 % categorized as Class 1, i.e., no vegetation is represented by red for NDVI and BNDVI, as shown in Fig. 14 (a) and (b), respectively. However, the NDRE index value in Fig. 14 (c) shows that >60 % of the area for the same rice plot is categorized in the same class. However, at 100 DAS, all plots recorded a better index value than the index value at 60 DAS.

Furthermore, a time-series analysis of the water level data that had been gathered for the period ranging from January 29 to February 6, 2021, in the studied area was also used to calibrate and validate the simulation findings from MIKE 21. The calibration graph for the time-series data of water levels simulated and collected using the tide gauge installed at Kuala Kedah Jetty, Malaysia, is seen in Fig. 15 (a) with the *RMSE* value at 6.74 %, which complies with the requirements of the guidelines issued by the Department of Irrigation and Drainage (DID), Malaysia. The same applies to the speed and direction values of the current which were also calibrated using the data modeled and observed in the study area, as depicted in Fig. 15 (b) and (c). The RMSE value for the current speed is 11.43 % while for the current direction is 18.7°. These two parameters also meet the requirements as stated in the DID guidelines of not >20 % and 20°, respectively, for the speed and direction of the current. Besides, the validation process was carried out based on the time series of speed and current direction of the observed data and the results of model simulations at ADCP1 and ADCP2 stations, as illustrated in Fig. 16a and b.

Thereafter, the coastal area of Kuala Kedah was divided into two parts, namely the northern part (NA) and the southern part (SA), for the simulation process using MIKE 21 Flow HD. The results of the K1 simulation showed that these two areas experienced coastal flooding due to rising sea levels between 2020, 2050 and 2100. Fig. 16 shows a forecast picture of areas affected by rising sea levels in 2012, 2020, 2050 and 2100. Visually, parts of SA are more affected than parts of NA from year to year in terms of the proximity of seawater to land and potentially flooded areas (Fig. 17).

Table 7 shows the maximum distance of seawater to mainland as a result of SLR for 2020, 2050 and 2100, from the simulations for K1 and K2. In 2012, for K1, the seawater advance distance to the mainland was expected to be up to a distance of 643.7 m and 788.5 m from the coastline and continued to increase to a distance of 926.5 m and 1212.6 m in 2100, respectively, for parts of NA and SA. However, the proximity of seawater to the mainland can be reduced taking into account the mitigation factors built by DID in 2016 in K2 modeling.

Table 7.

Fig. 18 shows the number of areas affected by the SLR in 2020, 2050 and 2100 for both conditions. In 2100, 469 ha and 498.9 ha are predicted to be flooded with the absence of coastal protection structures for parts of NA and SA, respectively. But if coastal protection structures are included in this flood analysis, the affected areas are expected to be reduced by up to 50 % even if these structures are only built in NA.

4. Discussion

Generally, during the 10 DAS period for both season and tidal events, the highest salinity concentration was seen in the downstream area of the Sungai Kedah estuary. There is a tidal gate that is commonly used to prevent seawater from entering nearby waters and also used to drain water from the highlands if it rains heavily (Walsh and Miskewitz, 2013). However, during heavy rainfall and high tides, the likelihood of seawater entering the river is very high due to rising sea levels. This causes higher salinity concentrations in this area (Fatema et al., 2016). In addition, during this period, the river was used directly for the purpose of irrigating the paddy crops in the area.

However, during the periods 40 DAS and 60 DAS, salinity concentrations were seen concentrated on the left side of Figs. 5 and 6 for both season and tide events. This area is located closest to the coastline and has the potential to indicate the penetration of seawater by overflow and underground movement through the pores of the soil particles while the area receives high rainfall. These results are consistent with a report by Geng and Boufadel (2017), which found that rain intensity significantly affects the salinity of pores near the coast. The movement of salinity particles to the supratidal zone occurs faster when receiving more rain at one time (Yu et al., 2020).

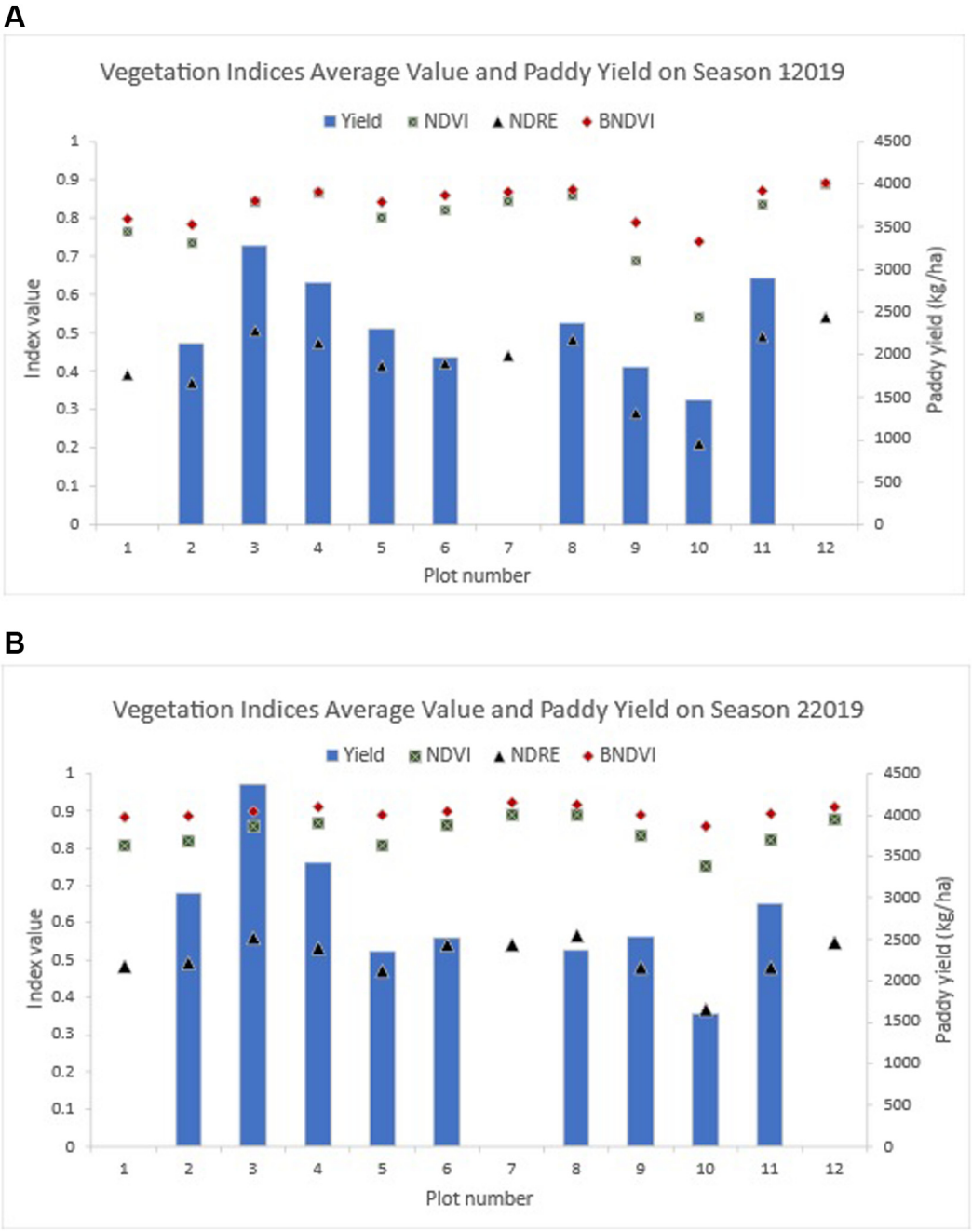

Fig. 11. Paddy yield and vegetation index (VI) by plot for (a) Season 1–2019 and (b) Season 2–2019.

Generally, the supratidal zone is known as a spray zone defined by a zone close to the coast but higher than the height of the tide. Sometimes this zone is splashed but not submerged by sea water (Darmawan et al., 2018). The zone is only flooded by seawater during high tide or the possibility of a large storm wave hitting the coastal zone. Therefore, the salinity concentration should be monitored and controlled to avoid losing the yield.

In addition, during Season 1–2019, the study area received a higher rainfall distribution and caused the rate of seawater distribution to the irrigation system higher; thus, resulting in an increase in salinity content in the crop plot especially at 10 DAS where higher rainfall was recorded compared to 40 and 60 DAS. The location of the study area in the supratidal zone received a high amount of seawater infiltration during heavy rains as the movement of salinity particles became faster and potentially flooded by seawater, as reported by Darmawan et al. (2018).

However, during Season 2–2019 with a small rainfall distribution, almost 100 % of the irrigation source was from river water especially at 60 DAS, which received the lowest rainfall compared to 10 and 40 DAS. During the tide incident in Season 2–2019, one sample point was found to record the highest salinity value of the season with 1160 ppm, which was due to backwater and reverse flow events. This is in line with the findings by Apel et al. (2020) and Sakai et al. (2021), which asserted that dry-season irrigation water tends to be saltier by the end of the 21st century due to the movement of seawater up to 80 km to the upstream part of the river during high tide events. Statistically, rainfall distribution has a significant difference on salinity concentration during Season 1–2019 and Season 2–2019 for both tidal events. Therefore, the concentration of salinity in this coastal area increases with rainfall intensity, which is influenced by the sea level during tidal occurrences.

As for the pH value, it was found that it was affected by the rainfall received where Season 1–2019 received a high amount of rainfall of up to 129 % compared to Season 2–2019 for both tidal events, as per Fig. 4. In addition, a report by Mama et al. (2021) stated that if there is a mixing of

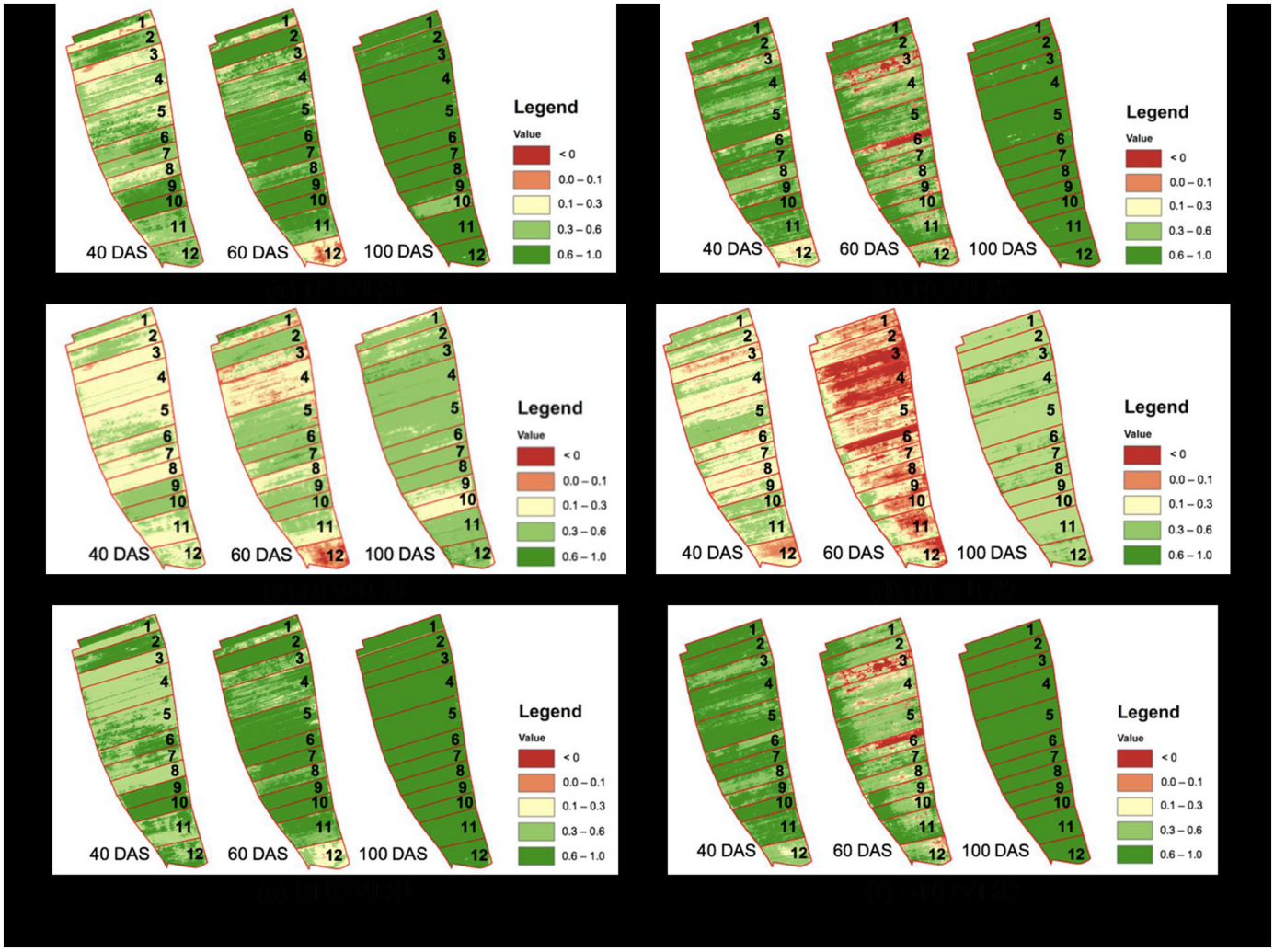

Fig. 12. Mapping of plant index for the entire study area for Season 1–2019 and Season 2–2019.

seawater and river water during the rainy season, the pH value will be somewhat higher than in the dry season. However, the pH values of both tidal events for Season 1–2019 and Season 2–2019 are within the normal range of pH values. This finding is in line with the normal range of pH values between 6 and 9 for the estuary area (Aurora et al., 2021). Whereas in terms of statistical analysis, salinity concentration has a very significant difference on the pH value of water for each tidal event for both seasons with a *p*-value lower than 0.0001.

Based on Fig. 10, it was found that a larger plot area did not necessarily produce higher rice yields than smaller plots. This is in line with the findings by Ceyhan et al. (2012) and Singh and Singh (2016), which stated that the yield of a crop is directly or indirectly influenced by a number of factors, especially environmental factors including water quality and proper agricultural practices. With the results from the use of the VI index through the spatial analysis approach, it is possible to translate the actual state of the crop.

Based on the statistical analysis of the rice and VI yield data in this study, as illustrated in Fig. 11, it shows that NDRE gives a more accurate value with the R-square value being 0.842 compared to 0.706 and 0.575, respectively, for the values of NDVI and BNDVI. These scenarios and findings are in line with the results of studies by Fu et al. (2020) and Zhang et al. (2019), which stated that NDRE is more stable than other plant indices. According to this diagram, the health of the paddy crop affects the amount of rice yield. It is noted that the high VI value, especially the NDRE value which has been proven to accurately reflect the state of a crop, will produce a high crop yield. This is because Red Edge and NIR are more sensitive and can characterize the dynamic growth of the canopy (Fu et al., 2020).

When this VI value is visualized as in Fig. 12, the NDRE value gives a more accurate picture than NDVI and BNDVI, as well as being validated with ground data, which is the yield of each paddy plot as shown in Fig. 11 (a) and (b). This situation is in line with the findings reported by Gholizadeh et al. (2017) in which NDRE has a high correlation with productivity values at 60 DAS for rice crops and corn crops as reported by Carvalho et al. (2020) due to the same characteristics and structure of leaves as rice (Islam et al., 2014).

In general, the analysis of each plot can be used to identify the problematic plot. Season 1–2019 shows an upward trend per VI, while Season 2–2019 is down at 60 DAS. This is due to surrounding factors such as low rainfall distribution which causes the salinity content in the paddy crop plot to be higher (Materu et al., 2018). However, at 10 DAS, the amount of water in the plant plot is released to ensure that the paddy grains reach maturity well and can be harvested at the right time. In terms of VI, NDRE shows a lower value compared to other VI as it is more sensitive to changes in chlorophyll content that affects the color of crop leaves (Fu et al., 2020; Lu et al., 2017; Simic Milas et al., 2018). However, the VI value shows a positive improvement which represents better crop conditions during this period.

Next, from the results of the hydrodynamic simulation for the K1 condition, more severe flooding is expected at the estuary of the Kedah River and the low surrounding areas of both the NA and SA areas. This is in line with findings by Awang et al. (2012) which discovered that sea level rise has the

A

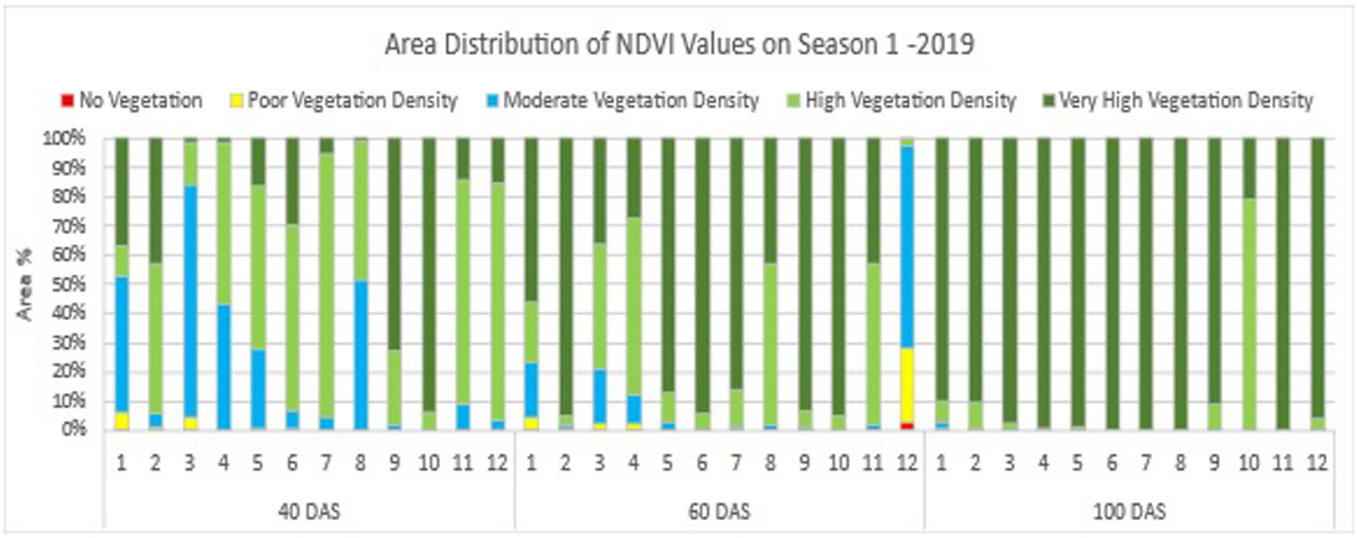

B

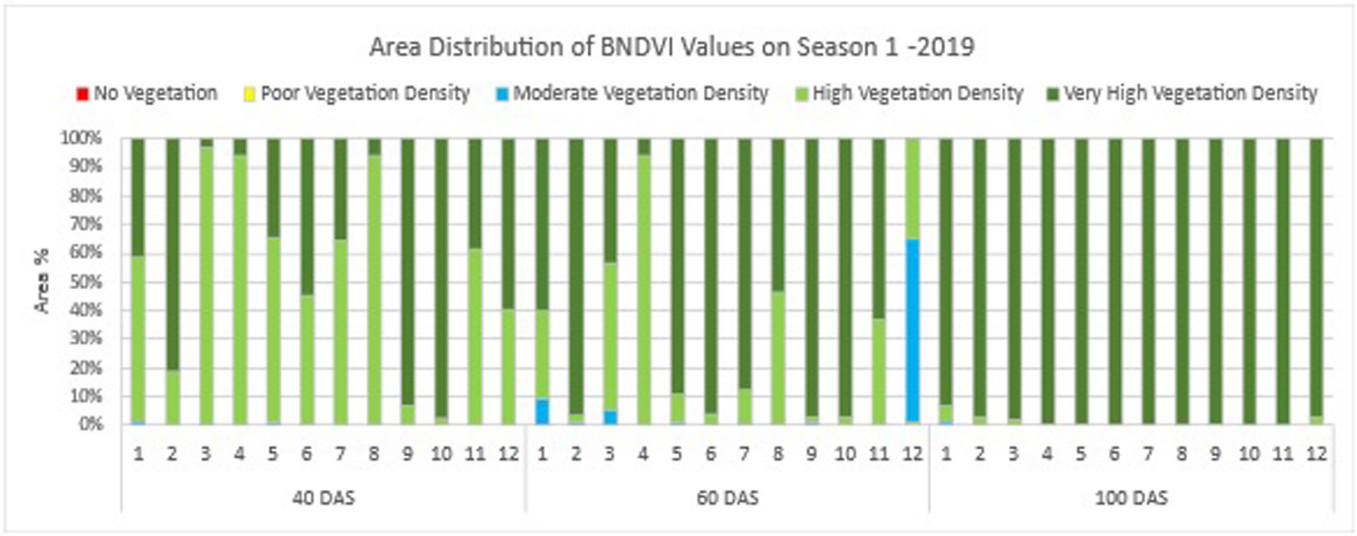

C

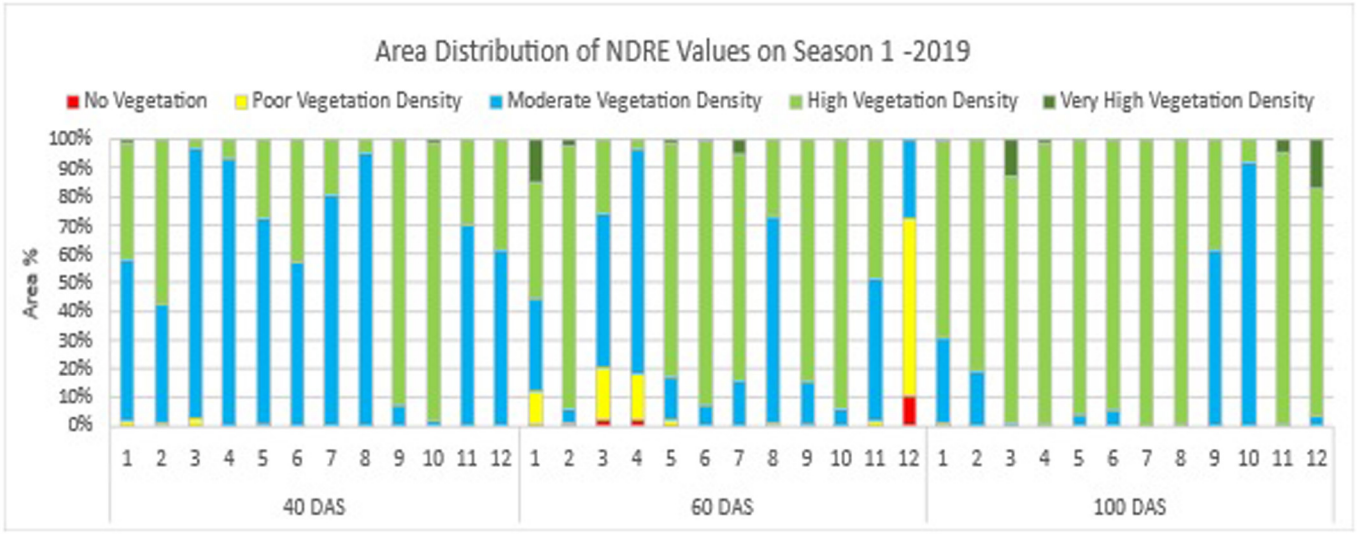

Fig. 13. Distribution of area by value category (a) NDVI, (b) BNDVI, and (c) NDRE during Season 1–2019.

A

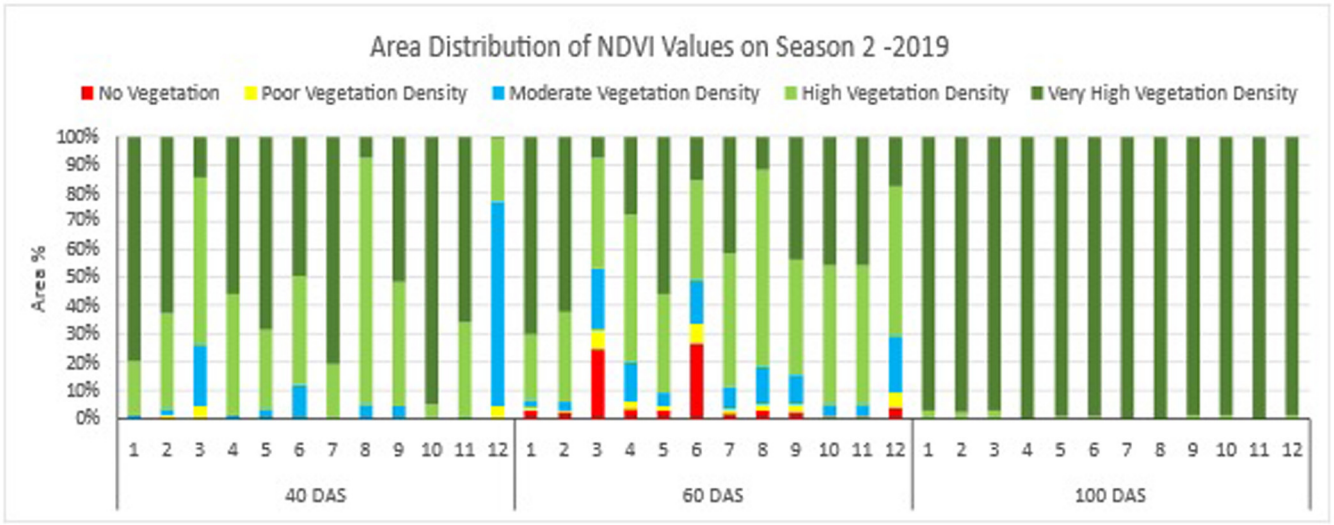

B

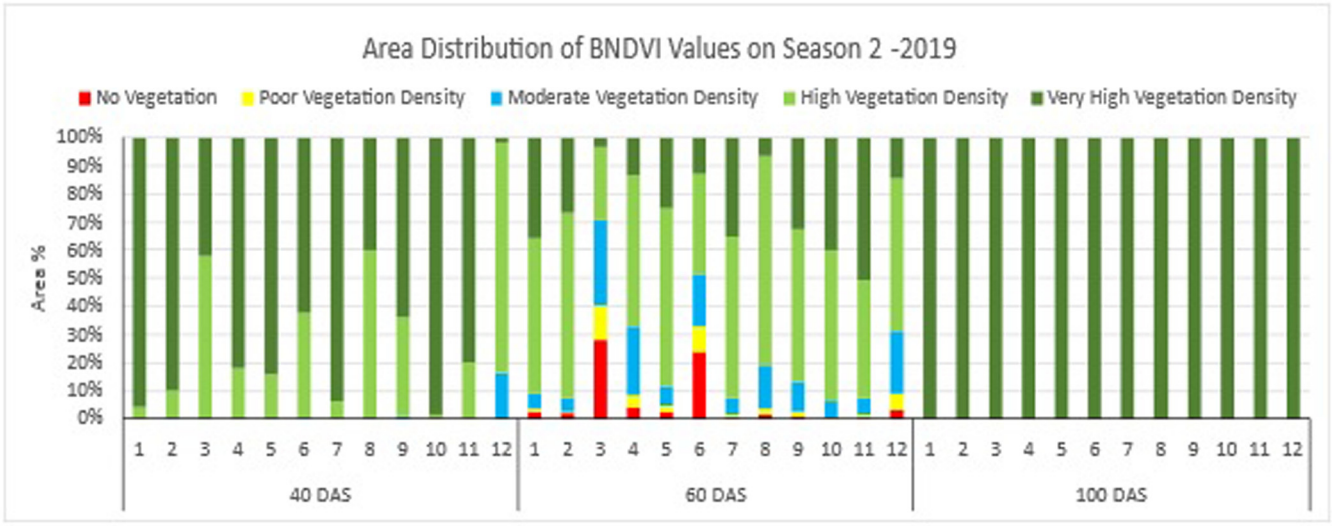

C

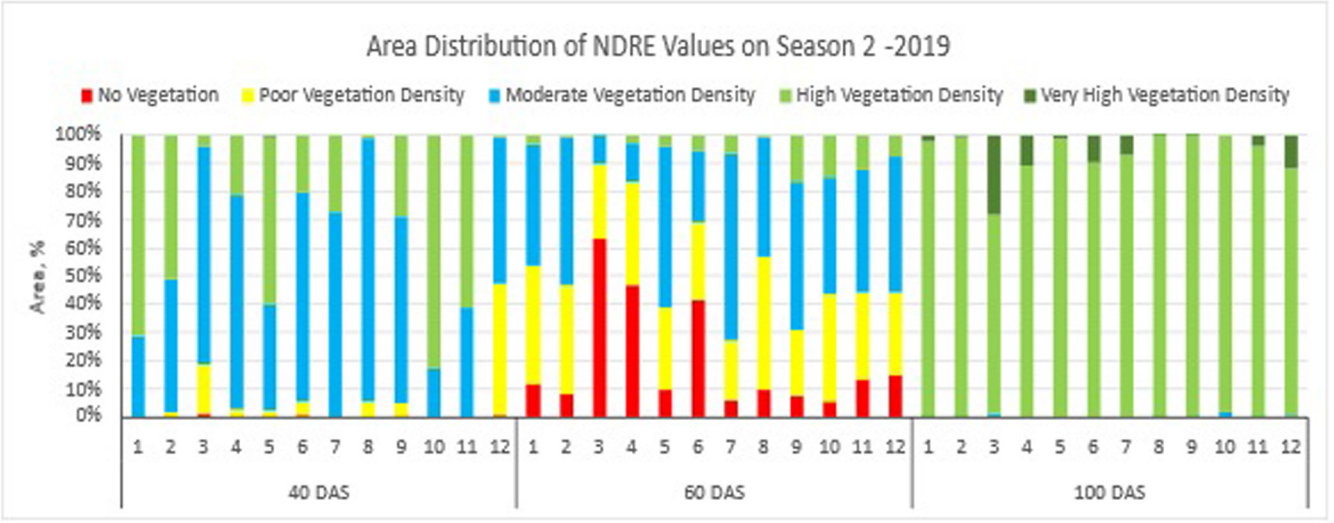

Fig. 14. Distribution of area by value category (a) NDVI, (b) BNDVI, and (c) NDRE during Season 2–2019.

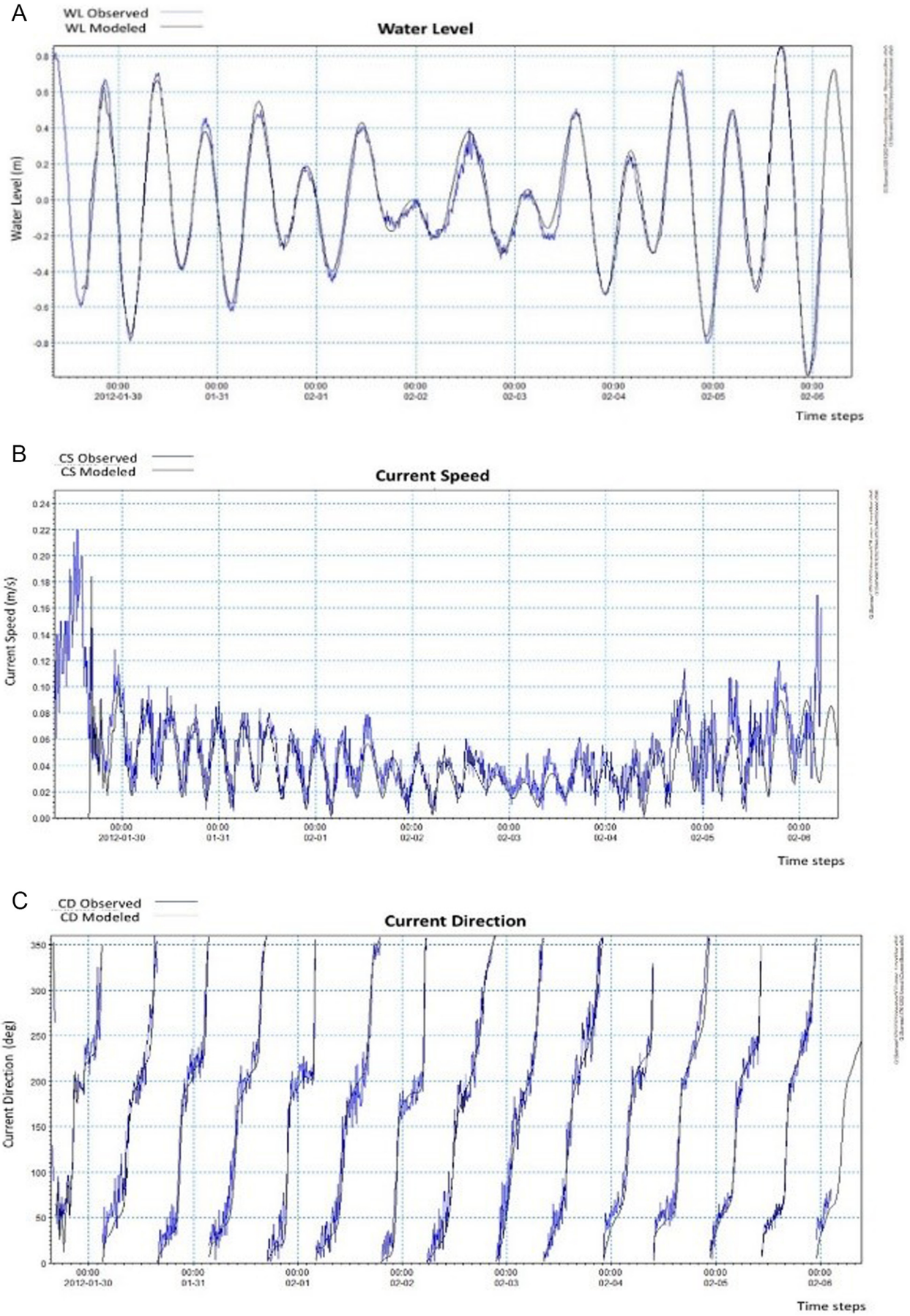

Fig. 15. Calibration graph for parameters (a) water level (b) current speed and (b) current direction.

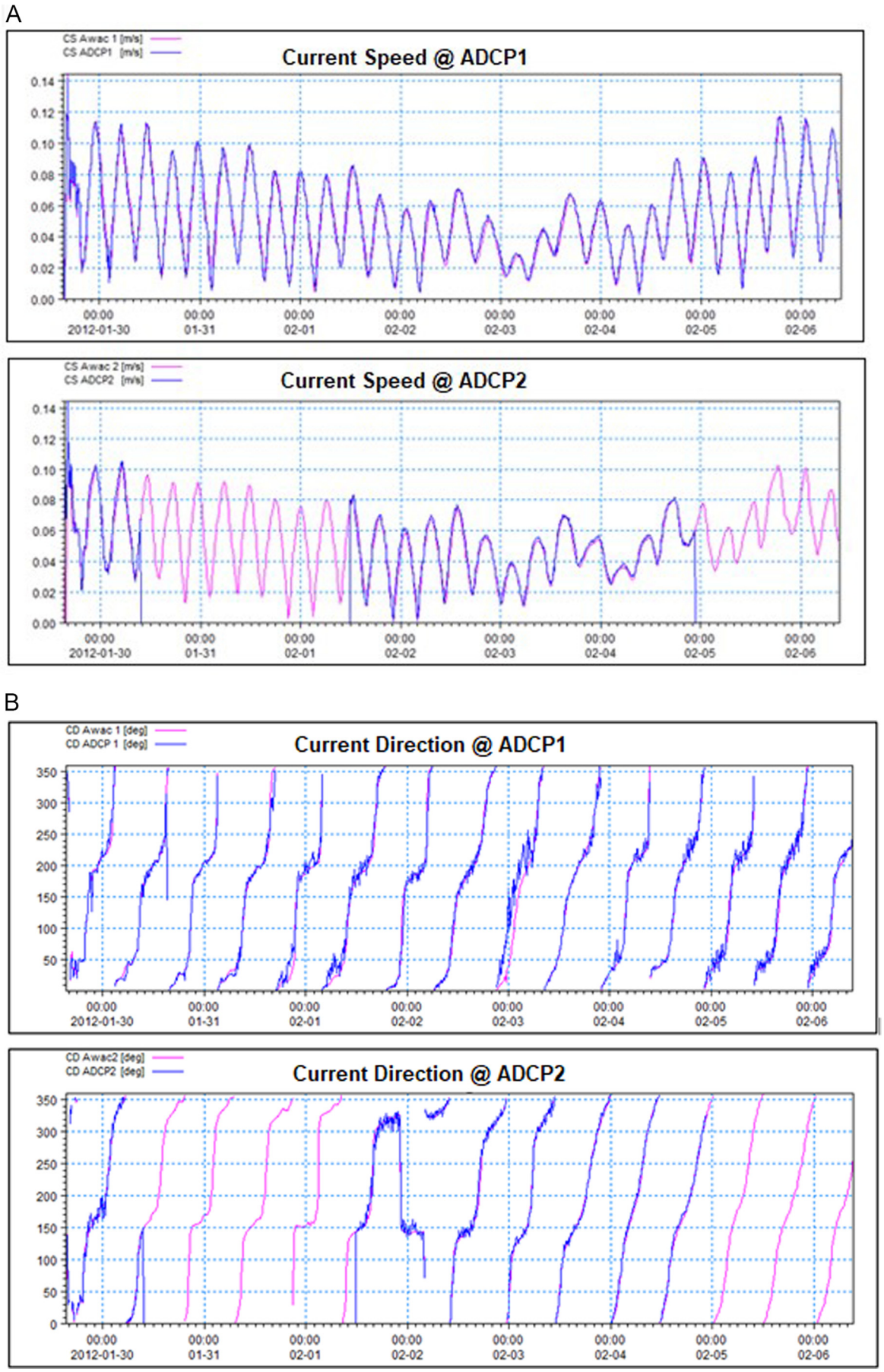

Fig. 16. Time series validation for (a) current speed and (b) current direction at ADCP1 and ADCP2.

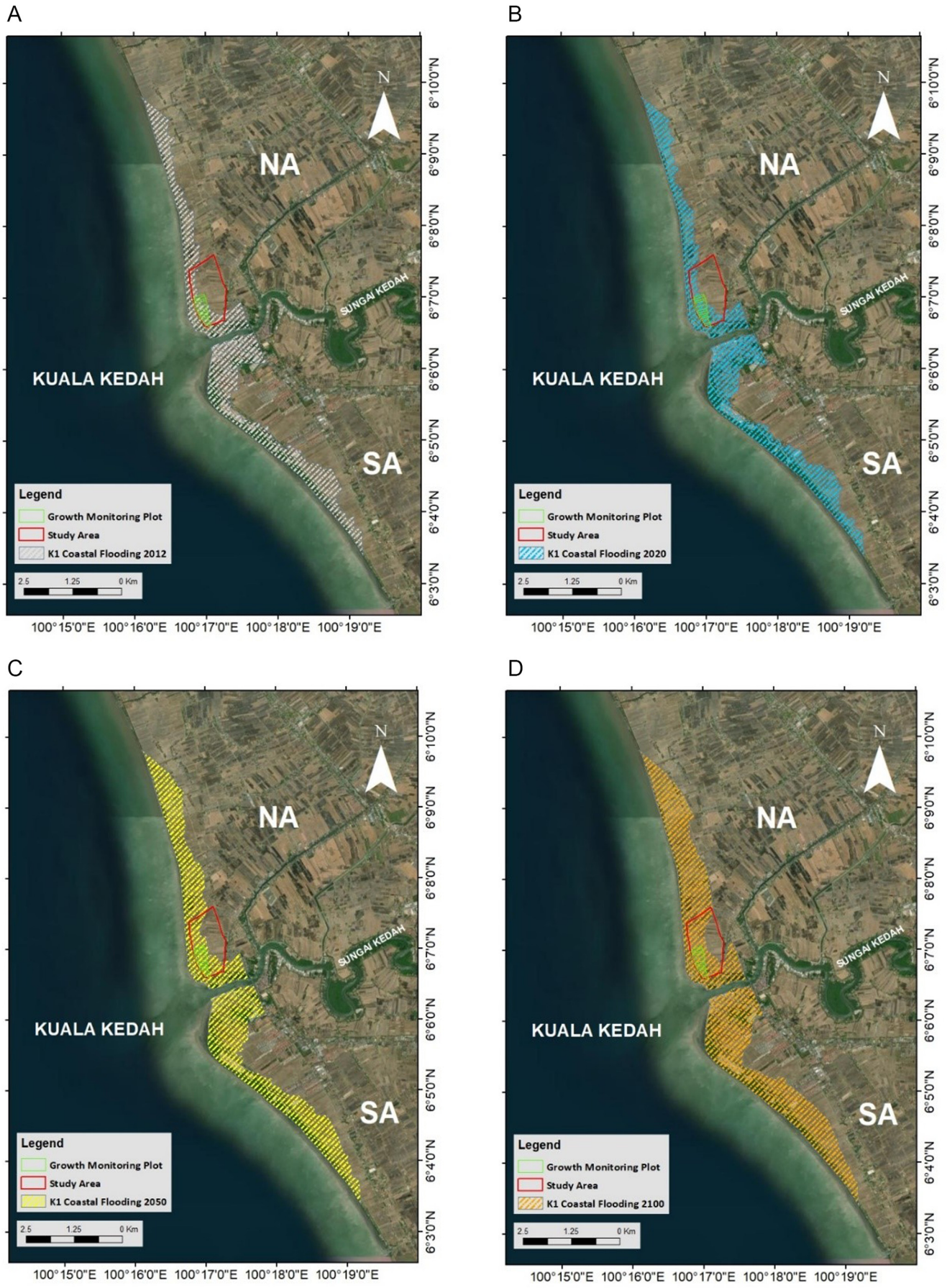

Fig. 17. Area of flooding K1 due to SLR for the year (a) 2012, (b) 2020, (c) 2050 and (d) 2100.

Table 7
Forecast of maximum distance of seawater advance to mainland due to SLR.

Year	K1 Distance (m)		K2 Distance (m)	
	NA	SA	NA	SA
2012	643.7	788.5	–	–
2020	752.7	810.6	586.4	717.5
2050	869.2	1123.8	690.1	879.8
2100	926.5	1212.6	759.9	960

Note: K1 = simulation without mitigation factor; K2 = simulation with mitigation factor; NA = northern area; SA = Southern area; Distance = distance from the coastline.

potential to submerge coastal areas and low estuaries, and could damage existing infrastructure and buildings. The results of a study by Mohd et al. (2018a, 2018b) also found that almost 1 km of buffer zone along the coast of Cherating to Pekan could potentially be flooded by the sea due to rising sea levels in the area.

For K2 conditions, the number of affected areas for the NA part can be reduced by >50 % compared to K1 conditions. However, the share of SA for K2 was only reduced by 10 % due to the absence of coastal protection structures in this part. Meanwhile, if measured in terms of the percentage of study areas affected by coastal floods in 2100, K2 recorded only 23 % compared to 72 % for K1 as illustrated in Fig. 18. The results of this analysis are consistent with the findings by Grases et al. (2020), Jahangirzadeh et al. (2012), and Zufayri Zulfakar et al. (2020) where coastal protection structures were found to be capable of absorbing high wave energy and reducing their impact as well as preventing seawater overflow due to overtopping waves and flooding during storm events.

Therefore, it is expected that in the year 2100, this seawater advance continues to be alarming not only to submerge the paddy planting area, but also the surrounding housing area if there are no permanent coastal protection structures in the mitigation plans in the future. Based on the total paddy yield for Season 1–2019 and Season 2–2019, on average each hectare produces 2.5 t of paddy and the total is estimated to be around 308 t loss per paddy season if 123 ha of paddy crop plot in this study area are entered by saltwater.

Overall, the results of this study can have a significant impact especially in the field of knowledge and society. It is seen that geospatial analysis is capable of translating various aspects and situations into the true picture; thus, expanding this field of knowledge to stakeholders. In addition, this study can also assist stakeholders in the planning and management of paddy crops as well as increase farmers' yields as recommended by the federal government.

5. Conclusion

The growth of paddy plants especially for areas located close to the coast depends on the level of water quality, especially the concentration of salinity and water pH which has a significant impact on the growth rate and health of the crop. However, the tidal variation of seawater should also be noted as it can affect the water quality level given the location of the paddy planting area which is located close to the coastline. Similarly, environmental conditions such as rainfall distribution play an important role in stabilizing the growth of crops and ecosystems. In addition, with the use of hydrodynamic modeling, it is able to support the findings of the study and in turn assist in identifying areas that are potentially affected by the increase in dynamic sea water levels over time. In conclusion, this integrated study was able to analyze and produce more comprehensive and detailed findings, especially to assess each element related to each other such as better water management, improve the health of plants especially for coastal areas, and directly improve the results. Therefore, the income of the farmers also increased, and thus, met the country's rice needs.

CRediT authorship contribution statement

Samera Samsuddin Sah: Conceptualization, Methodology, Writing-Original draft preparation, Software, Validation. **Khairul Nizam Abdul Maulud:** Conceptualization, Writing- Reviewing and Editing, Supervision, Data curation, Validation, Visualization, Investigation, Funding acquisition.

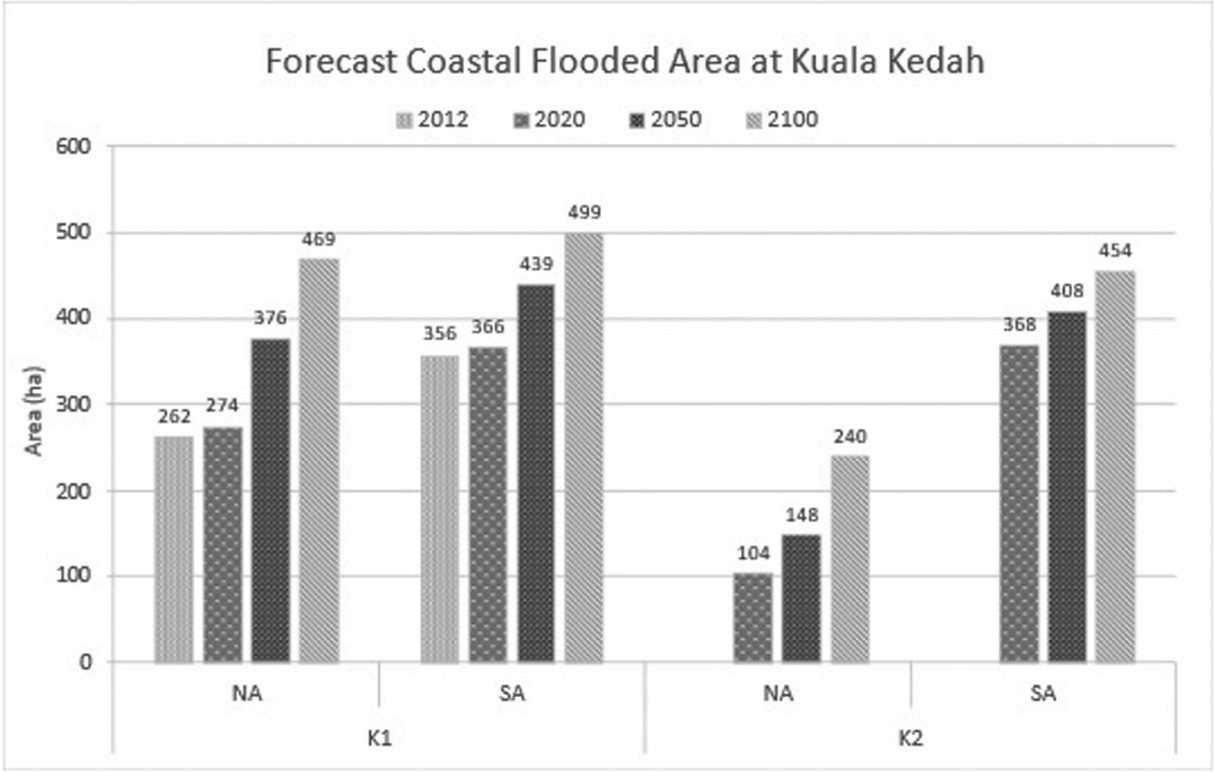

Fig. 18. Forecast of areas affected by SLR.

Othman A. Karim: Writing- Reviewing and Editing, Validation. **Suraya Sharil:** Writing- Reviewing and Editing, Validation. **Zaher Mundher Yaseen:** Writing- Reviewing and Editing, Validation.

Data availability

Data will be made available on request.

Declaration of competing interest

The authors declare the following financial interests/personal relationships which may be considered as potential competing interests: Khairul Nizam Abdul Maulud reports financial support was provided by Faculty of Engineering and Built Environment, Universiti Kebangsaan Malaysia.

Acknowledgement

The authors would like to thank Universiti Kebangsaan Malaysia and the UKM-YSD Chair for funding this study under the UKM YSD Chair in Sustainability, UKM-YSD-2021-003 and the Dana Impak Perdana grant, DIP-2021-006, respectively.

References

Abd Rahim, N.A., Abdul Maulud, K.N., Mohd, F.A., Lee, L.H., Wan Mohtar, W.H.M., 2021. Evaluation of coastal hydrodynamic performance using statistical analysis at the Kelantan coast, Malaysia. Malaysian Journal of Society and Space 17 (4). https://doi.org/10.17576/geo-2021-1704-27.

Abrol, I.P., Yadav, J.S.P., Massoud, F.I., 1988. Soils-affected soils and their management. FAO Soils Bulletin. 39. FAO, Rome.

Ahmed, M.F., Haider, M.Z., 2014. Impact of salinity on rice production in the south-west region of Bangladesh. Environmental Science 9 (4), 135–141. https://doi.org/10.4135/9781446247501.n1321.

Apel, H., Khiem, M., Hong Quan, N., Quang Toan, T., 2020. Brief communication: seasonal prediction of salinity intrusion in the Mekong Delta. Nat. Hazards Earth Syst. Sci. 20 (6), 1609–1616. https://doi.org/10.5194/nhess-20-1609-2020.

Aurora, M.R., Ward, M., Tessa, M.H., Sanford, E., Kristy, J.K., Yuichiro, T., Sarah, M., Priya, S., Aaron, T.N., Elsmore, K., Brian, G., 2021. Coast- wide evidence of low pH amelioration by seagrass ecosystems. Glob. Chang. Biol. 27, 2580–2591. https://doi.org/10.1111/gcb.15594.

Awang, N.A., Lee, H.L., Wan Jusoh, W.H., Ahmad, A., 2012. Desktop study for inundation of Kedah estuary - impact of sea level rise due to climate change. Malaysia Water Res. J. 2 (1), 65–74.

Baten, M.A., Seal, L., Lisa, K.S., 2015. Salinity intrusion in interior coast of Bangladesh: challenges to agriculture in south-central coastal zone. Am. J. Clim. Chang. 04, 248–262. https://doi.org/10.4236/ajcc.2015.43020.

Belibassakis, K.A., Karathanasi, F.E., 2017. Modelling nearshore hydrodynamics and circulation under the impact of high waves at the coast of varkiza in saronic-Athens gulf. Oceanologia 59, 350–364. https://doi.org/10.1016/j.oceano.2017.04.001.

Buschmann, C., Nagel, E., 1993. In vivo spectroscopy and internal optics of leaves as basis for remote sensing of vegetation. Int. J. Remote Sens. 14 (4), 711–722. https://doi.org/10.1080/01431169308904370.

Carvalho, L.F.D.de, Amado, T.J.C., Sobrinho, J.C., Pott, L.P., Piccin, M., Amaral, L.de P., Pedron, V.F., 2020. Nutritional status of corn plants estimated through different vegetation indices in the growth stages. Rev. Engenharia Agric. Reveng 28 (October), 255–264. https://doi.org/10.13083/reveng.v28i.8564.

Ceyhan, E., Kahraman, A., Onder, M., 2012. The impacts of environment on plant products. Int. J. Biosci. Biochem. Bioinform. 2 (1), 48–51. https://doi.org/10.7763/ijbbb.2012.v2.68.

Cheng, Q., Jianrong, Z., Yuliang, G., 2012. Impact of seasonal tide variation on saltwater intrusion in the Changjiang River estuary. Chin. J. Oceanol. Limnol. 30 (2), 342–351. https://doi.org/10.1007/s00343-012-1115-x.

Dam, T.H.T., Amjath-Babu, T.S., Bellingrath-Kimura, S., Al, E., 2019. The impact of salinity on paddy production and possible varietal portfolio transition: a Vietnamese case study. Paddy Water Environ. 17 (4), 771–782. https://doi.org/10.1007/s10333-019-00756-9.

Darmawan, A., Saputra, D.K., Wiadnya, D.G.R., Gusmida, A.M., 2018a. Prediction of supratidal zones as turtle nesting sites using remote sensing and geographic information system, a case study in pacitan, southern Java Sea. IOP Conf. Ser.: Earth Environ. Sci. 137. https://doi.org/10.1088/1755-1315/137/1/012091.

Department of Agriculture Malaysia, 2020. Crop statistics booklet (Food crops sub-Sector). http://www.doa.gov.my/index.php/pages/view/622?mid=239.

Department of Irrigation and Drainage Malaysia, 2013. Guidelines for Preparation of Coastal Engineering Hydraulic Study and Impact Evaluation. DID, Malaysia. https://www.water.gov.my/jps/resources/Guidelines_for_Hydraulics_Studies.pdf.

Department of Town and Country Planning Malaysia, 2018. Booklet Kompendium PLANMalaysia. . https://www.planmalaysia.gov.my/kompendium/booklet/Booklet_Keluaran_1.pdf.

Fatema, K., Omar, W., Isa, M., 2016. Effects of tidal events on the water quality in the Merbok estuary, Kedah, Malaysia. J. Environ. Sci. Nat. Resour. 8 (2), 15–19. https://doi.org/10.3329/jesnr.v8i2.26858.

Fattah, A.H., Suntoyo, Damerianne, H. A., amp, Wahyudi., 2018. Hydrodynamic and sediment transport modelling of suralaya coastal area, Cilegon, Indonesia. IOP Conf. Ser.: Earth Environ. Sci. 135 (1), 0–9. https://doi.org/10.1088/1755-1315/135/1/012024.

Fraga, T.I., Carmona, F.D.C., Anghinoni, I., 2010. Flooded Rice yield as affected by levels of water salinity in different stages of its cycle. Braz. J. Soil. Sci. 34, 175–182. https://doi.org/10.1590/S0100-06832010000100018.

Fu, Z., Jiang, J., Gao, Y., Krienke, B., Wang, M., Zhong, K., Cao, Q., Tian, Y., Zhu, Y., Cao, W., Liu, X., 2020. Wheat growth monitoring and yield estimation based on multi-rotor unmanned aerial vehicle. Remote Sens. 12, 508. https://doi.org/10.3390/rs12030508.

Gain, P., Mannan, M.A., Pal, P.S., Hossain, M.M., Parvin, S., 2004. Effect of salinity on some yield attributes of Rice. Pak. J. Biol. Sci. 7, 760–762. https://doi.org/10.3923/pjbs.2004.760.762.

Garcés-Vargas, J., Schneider, W., Pinochet, A., Piñones, A., Olguin, F., Brieva, D., Wan, Y., 2020. Tidally forced saltwater intrusions might impact the quality of drinking water, the Valdivia River (40° S). Chile Estuary Case. Water 12, 2387. https://doi.org/10.3390/w12092387.

Geng, X., Boufadel, M.C., 2017. The influence of evaporation and rainfall on supratidal groundwater dynamics and salinity structure in a sandy beach. Water Resour. Res. 53, 6218–6238. https://doi.org/10.1002/2016WR020344.

Gholizadeh, A., Saberioon, M., Borůvka, L., Wayayok, A., Mohd Soom, M.A., 2017. Leaf chlorophyll and nitrogen dynamics and their relationship to lowland rice yield for site-specific paddy management. Inf. Process. Agric. 4, 259–268. https://doi.org/10.1016/j.inpa.2017.08.002.

Giacomo, R., David, G., 2018. E-agriculture in action: drones for agriculture. In: Sylvester, G. (Ed.), Food and Agriculture Organization of the United Nations and International Telecommunication Union. FAO and ITU , pp. 9–25.. http://www.fao.org/3/i8494en/i8494en.pdf.

Glock, K., Tritthart, M., Habersack, H., Hauer, C., 2019. Comparison of hydrodynamics simulated by 1D, 2D and 3D models focusing on bed shear stresses. Water 11, 226. https://doi.org/10.3390/w11020226.

Grases, A., Gracia, V., García-León, M., Lin-Ye, J., Sierra, J.P., 2020. Coastal flooding and erosion under a changing climate: implications at a low-lying coast (ebro delta). Water 12, 346. https://doi.org/10.3390/w12020346.

Grieve, C.M., Grattan, S.R., Maas, E.V., 2012. Plant salt tolerance. In: Wallender, W.W., Tanji, K.K. (Eds.), Agricultural Salinity Assessment and Management, 2nd ed. American Society of Civil Engineers, Reston, VA, USA, pp. 405–459 https://doi.org/10.1061/9780784411698.ch13.

Hashim, H., Abd Latif, Z., Adnan, N.A., 2019. Urban vegetation classification with Ndvi threshold value method with very high resolution (Vhr) pleiades imagery. 6th International Conference on Geomatics and Geospatial Technology, XLII-4/W16, pp. 237–240 https://doi.org/10.5194/isprs-archives-xlii-4-w16-237-2019.

Herman, T., Murchie, E.H., Warsi, A.A., 2015. Rice production and climate change: a case study of Malaysian rice. Pertanika J. Trop. Agric. Sci. 38 (3), 321–328.

Huete, A., Didan, K., Rodriguez, E.P., Gao, X., Ferreira, L.G., 2002. Overview of the radiometric and biophysical performance of the MODIS vegetation indices. Remote Sens. Environ. 83, 195–213. https://doi.org/10.1016/S0034-4257(02)00096-2.

Iglesias, I., Avilez-Valente, P., Pinho, J.L., Bio, A., Vieira, J.M., Bastos, L., Veloso-Gomes, F., 2019. Numerical modeling tools applied to estuarine and coastal hydrodynamics: a user perspective. Coastal and Marine Environments - Physical Processes and Numerical Modelling. IntechOpen https://doi.org/10.5772/intechopen.85521.

Islam, M.R., Haque, K.M.S., Akter, N., Karim, M.A., 2014. Leaf chlorophyll dynamics in wheat based on SPAD meter reading and its relationship with grain yield. Sci. Agric. 8 (1), 13–18. https://doi.org/10.15192/pscp.sa.2014.4.1.1318.

Jahangirzadeh, A., Akib, S., Kamali, B., Shamsudin, S., Kimiaei, K., 2012. Effects of construction of coastal structure on ecosystem. World Acad. Sci. Eng. Technol. 65, 663–674.

Jesslyn, B., 2015. NDVI, the Foundation for Remote Sensing Phenology. U.S. Geological Survey (USGS). https://www.usgs.gov/land-resources/eros/phenology/science/ndvi-foundation-remote-sensing-phenology?qt-science_center_objects=0#qt-science_center_objects.

Kahimba, F.C., Ali, R.M., Mahoo, H.F., 2016. Evaluation of irrigation water quality for paddy production at Bumbwisudi Rice Irrigation Scheme, Zanzibar. Tanzania Journal of Agricultural Sciences 15 (2), 114–119.

Kamruzzaman, M., Hwang, S., Choi, S.K., Cho, J., Song, I., Song, J.H., Jeong, H., Jang, T., Yoo, S.H., 2020. Evaluating the impact of climate change on paddy water balance using APEX-paddy model. Water 12 (3), 1–20. https://doi.org/10.3390/w12030852.

Khanom, T., 2016. Effect of salinity on food security in the context of interior coast of Bangladesh. Ocean Coast. Manag. 130, 205–212. https://doi.org/10.1016/j.ocecoaman.2016.06.013.

Khojasteh, D., Hottinger, S., Felder, S., De Cesare, G., Heimhuber, V., Hanslow, D.J., Glamore, W., 2020. Estuarine tidal response to sea level rise: the significance of entrance restriction. Estuar. Coast. Shelf Sci. 244, 106941. https://doi.org/10.1016/j.ecss.2020.106941.

Liu, X., Tao, Y., Wen, G., Kong, F., Zhang, X., Hu, Z., 2016. Influence of soil and irrigation water ph on the availability of phosphorus in struvite derived from urine through a greenhouse pot experiment. J. Agric. Food Chem. 64 (17), 3324–3329. https://doi.org/10.1021/acs.jafc.6b00021.

Liu, B., Liu, H., Cao, W., Tian, Y., Cheng, T., Yao, X., Zhu, Y., Cao, Z., 2019. Comparison of the abilities of vegetation indices and photosynthetic parameters to detect heat stress in wheat. Agric. For. Meteorol. 265, 121–136. https://doi.org/10.1016/j.agrformet.2018.11.009.

Lu, X., Zhuang, Q., 2010. Evaluating evapotranspiration and water-use efficiency of terrestrial ecosystems in the conterminous United States using MODIS and AmeriFlux data. Remote Sens. Environ. 114 (9), 1924–1939. https://doi.org/10.1016/j.rse.2010.04.001.

Lu, J., Miao, Y., Shi, W., Li, J., Yuan, F., 2017. Evaluating different approaches to nondestructive nitrogen status diagnosis of rice using portable RapidSCAN active canopy sensor. Sci. Rep. 7 (1), 1–10. https://doi.org/10.1038/s41598-017-14597-1.

Maghrebi, M., Noori, R., Bhattarai, R., Mundher Yaseen, Z., Tang, Q., Al-Ansari, N., Danandeh Mehr, A., Karbassi, A., Omidvar, J., Farnoush, H., Torabi Haghighi, A., Kløve, B., Madani, K., 2020. Iran's agriculture in the anthropocene. Earth's Future https://doi.org/10.1029/2020EF001547.

Mama, A.C., Bodo, W.K.A., Ghepdeu, G.F.Y., Ajonina, G.N., Ndam, J.R.N., 2021. Understanding seasonal and spatial variation of water quality parameters in mangrove estuary of the Nyong River using multivariate analysis (Cameroon southern Atlantic Coast). Open J. Mar. Sci. 11 (03), 103–128. https://doi.org/10.4236/ojms.2021.113008.

Materu, S.T., Shukla, S., Sishodia, R.P., Tarimo, A., Tumbo, S.D., 2018. Water use and rice productivity for irrigation management alternatives in Tanzania. Water (Switzerland) 10 (8), 1–15. https://doi.org/10.3390/w10081018.

McCauley, A., Jones, C., Olson-Rutz, K., 2017. Module 8: soil pH and organic matter. Nutrient Management. 4449–8 , pp. 1–16.. https://www.certifiedcropadviser.org/files/certifications/certified/education/self-study/exam-pdfs/38.pdf.

Migliavacca, M., Simmer, C., van der Tol, C., Schneider, F.D., Morsdorf, F., Paul-Limoges, E., Damm, A., Rascher, U., Haghighi, E., 2018. Remote sensing of plant-water relations: an overview and future perspectives. J. Plant Physiol. 227, 3–19. https://doi.org/10.1016/j.jplph.2018.04.012.

Mohd, F.A., Abdul Maulud, K.N., Karim, O.A., Ibrahim, M.A.F.I., Benson, Y.A., Abd Wahab, A.K., 2018. Integrasi Kaedah Geospatial dan Pemodelan Hidrodinamik untuk Mengkaji Impak Kenaikan Aras Laut Terhadap Kawasan Pantai. Jurnal Kejuruteraan 30 (1), 65–75. https://doi.org/10.17576/jkukm-2018-30(1).

Mohd, F.A., Maulud, K.N.A., Karim, O.A., Begum, R.A., Awang, N.A., Hamid, M.R.A., Rahim, N.A.A., Abd Razak, A.H., 2018. Assessment of coastal inundation of low lying areas due to sea level rise. IOP conf. Series: earth and environmentalScience 169 (012046). https://doi.org/10.1088/1755-1315/169/1/012046.

Neill, S.P., Hashemi, M.R., 2018. Chapter 8 - ocean modelling for resource characterization. Fundamentals of Ocean Renewable Energy, pp. 193–235 https://doi.org/10.1016/b978-0-12-810448-4.00008-2.

Norasma, C.Y.N., Sari, M.A., Fadzilah, M.A., Ismail, M.R., Omar, M.H., Zulkarami, B., Hassim, Y.M.M., Tarmidi, Z., 2018. Rice crop monitoring using multirotor UAV and RGB digital camera at early stage of growth. IOP conf. Series: earth and environmentalScience 169 (012095). https://doi.org/10.1088/1755-1315/169/1/012095.

Parsapour-moghaddam, P., Rennie, C.D., Slaney, J., 2018. Hydrodynamic simulation of an irregularly meandering gravel-Bed River: comparison of MIKE 21 FM and Delft3D flow models. E3S Web of Conferences. 40, pp. 1–8. https://doi.org/10.1051/e3sconf/20184002004.

Phogat, V., Yadav, A.K., Malik, R.S., Kumar, S., Cox, J., 2010. Simulation of salt and water movement and estimation of water productivity of rice crop irrigated with saline water, pp. 333–346 https://doi.org/10.1007/s10333-010-0213-7.

Prince, R., 2019. Water salinity and plant irrigation Direct adsorption through leaves. Department of Primary Industries and Regional Development's Agriculture and Food Australia.

Radanielson, A.M., Gaydon, D.S., Li, T., Angeles, O., Roth, C.H., 2018a. Modeling salinity effect on rice growth and grain yield with ORYZA v3 and APSIM-oryza. Eur. J. Agron. 100, 44–55. https://doi.org/10.1016/j.eja.2018.01.015.

Radanielson, A.M., Gaydon, D.S., Li, T., Angeles, O., Roth, C.H., 2018. Modeling salinity effect on rice growth and grain yield with ORYZA v3 and APSIM-Oryza. 100 (March), 44–55. https://doi.org/10.1016/j.eja.2018.01.015.

Reddy, I.N.B.L., Kim, B.-K., Yoon, I.-S., Kim, K.-H., Kwon, T.-R., 2017. Salt tolerance in Rice: focus on mechanisms and approaches. Rice Sci. 24 (3), 123–144. https://doi.org/10.1016/j.rsci.2016.09.004.

Rouse, J.W., Hass, R.H., Schell, J.A., Deering, D.W., 1973. Monitoring vegetation systems in the great plains with ERTS. Third Earth Resources Technology Satellite (ERTS) Symposium. 1, pp. 309–317 (https://doi.org/citeulike-article-id:12009708).

Sakai, T., Omori, K., Oo, A.N., Zaw, Y.N., 2021. Monitoring saline intrusion in the Ayeyarwady Delta, Myanmar, using data from the Sentinel-2 satellite mission. Paddy Water Environ. 19 (2), 283–294. https://doi.org/10.1007/s10333-020-00837-0.

Salman, S.A., Shahid, S., Sharafati, A., Salem, G.S.A., Bakar, A.A., Farooque, A.A., Chung, E.S., Ahmed, Y.A., Mikhail, B., Yaseen, Z.M., 2021. Projection of agricultural water stress for climate change scenarios: a regional case study of Iraq. Agriculture (Switzerland) 11 (12), 1288. https://doi.org/10.3390/agriculture11121288.

Simic Milas, A., Romanko, M., Reil, P., Abeysinghe, T., Marambe, A., 2018. The importance of leaf area index in mapping chlorophyll content of corn under different agricultural treatments using UAV images. Int. J. Remote Sens. 39 (15–16), 5415–5431. https://doi.org/10.1080/01431161.2018.1455244.

Singh, H., Singh, R.K., 2016. Environmental Factors Affecting Growth and Productivity of. November. https://doi.org/10.13140/RG.2.2.16576.58882.

Suárez-López, M.J., Espina-Valdés, R., Pacheco, V.M.F., Manso, A.N., Blanco-Marigorta, E., Álvarez-Álvarez, E., 2019. A review of software tools to study the energetic potential of tidal currents. Energies 12 (9). https://doi.org/10.3390/en12091673.

Symonds, A.M., Vijverberg, T., Post, S., Van der Spek, B.-J., Henrotte, J., Sokolewicz, M., 2017. Comparison between Mike 21 fm, Delft3D and Delft3D fm flow models of Western Port BayAustralia. Coastal Engineering Proceedings 35, 11. https://doi.org/10.9753/icce.v35.currents.11.

Tack, J., Singh, R.K., Nalley, L.L., Viraktamath, B.C., Krishnamurthy, S.L., Lyman, N., Jagadish, K.S.V., 2015. High vapor pressure deficit drives salt-stress-induced rice yield losses in India. Glob. Chang. Biol. 21 (4), 1668–1678. https://doi.org/10.1111/gcb.12803.

Thu, T.T.P., Yasui, H., Yamakawa, T., 2017. Effects of salt stress on plant growth characteristics and mineral content in diverse rice genotypes. Soil Sci. Plant Nutr. 63 (3), 264–273. https://doi.org/10.1080/00380768.2017.1323672.

Uncles, R.J., Stephens, J.A., 2011. The effects of wind, runoff and tides on salinity in a strongly tidal sub-estuary. Estuar. Coasts 34, 758–774. https://doi.org/10.1007/s12237-010-9365-3.

USDA, 1994. Inherent Factors Affecting Soil Phosphorus (Issue Figure 1).

Walsh, S., Miskewitz, R., 2013. Impact of sea level rise on tide gate function. J. Environ. Sci. Health A Tox. Hazard. Subst. Environ. Eng. 48 (4), 453–463. https://doi.org/10.1080/10934529.2013.729924.

Wang, F., Huang, J., Tang, Y., Wang, X., 2007. New vegetation index and its application in estimating leaf area index of Rice. Rice Sci. 14 (3), 195–203. https://doi.org/10.1016/s1672-6308(07)60027-4.

Xiao, W., Xu, S., He, T., 2021. Mapping paddy rice with sentinel-1/2 and phenology-, object-based algorithm—a implementation in Hangjiahu Plain in China using GEE platform. Remote Sensing 13 (990). https://doi.org/10.3390/rs13050990 Academic.

Yebra, M., Van Dijk, A., Leuning, R., Huete, A., Guerschman, J.P., 2013. Evaluation of optical remote sensing to estimate actual evapotranspiration and canopy conductance. Remote Sens. Environ. 129, 250–261. https://doi.org/10.1016/j.rse.2012.11.004.

Yeom, J.M., Jeong, S., Deo, R.C., Ko, J., 2021. Mapping rice area and yield in northeastern Asia by incorporating a crop model with dense vegetation index profiles from a geostationary satellite. GIScience Remote Sens. 58 (1), 1–27. https://doi.org/10.1080/15481603.2020.1853352.

Yu, X., Zhan, C., Wu, M., Niu, X., Zhang, X., Wang, Q., Cui, B., 2020. An improved method for mapping tidal waterways based on remotely sensed waterlines: a case study in the Yellow River DeltaChina. Marine Georesources and Geotechnology 38 (8), 887–895. https://doi.org/10.1080/1064119X.2019.1640321.

Zaitunah, A., Samsuri, Ahmad, A. G., amp, Safitri, R.A., 2018. Normalized difference vegetation index (ndvi) analysis for land cover types using landsat 8 oli in besitang watershed, Indonesia. IOP Conference Series: Earth and Environmental Science 126 (012112). https://doi.org/10.1088/1755-1315/126/1/012112.

Zhang, G., Xiao, X., Biradar, C.M., Dong, J., Qin, Y., Menarguez, M.A., Zhou, Y., Zhang, Y., Jin, C., Wang, J., Doughty, R.B., Ding, M., Moore, B., 2017. Spatiotemporal patterns of paddy rice croplands in China and India from 2000 to 2015. Sci. Total Environ. 579, 82–92. https://doi.org/10.1016/j.scitotenv.2016.10.223.

Zhang, K., Ge, X., Shen, P., Li, W., Liu, X., Cao, Q., Zhu, Y., Cao, W., Tian, Y., 2019. Predicting rice grain yield based on dynamic changes in vegetation indexes during early to mid-growth stages. Remote Sens. 11 (4). https://doi.org/10.3390/rs11040387.

Zufayri Zulfakar, M.S., Akhir, M.F., Ariffin, E.H., Awang, N.A., Yaacob, M.A.M., Chong, W.S., Muslim, A.M., 2020. The effect of coastal protections on the shoreline evolution at kuala nerus, Terengganu (Malaysia). J. Sustain. Sci. Manag. 15 (3), 71–85.